Journal of Operation and Automation in Power Engineering

Vol. 14, No. 1, Jan. 2026, Pages: 1-19

http://joape.uma.ac.ir

Research Paper

Multi-Objective Optimization for Day-Ahead HT-WP-PV-PSH with LS-EVs Systems Self-Scheduling Unit Commitment Using HHO-PSO Algorithm

Mohammad Reza Behnamfar [1, *], *Hassan Barati* [2], *Mahyar Abasi* [3, 4], *Mohammad Alaleh* [1], and *Gholam Ali Torabi* [1]

[1]*Khuzestan Regional Electric Company (KZREC), Ahvaz, Iran.*
[2]*Department of Electrical Engineering, Dezful Branch, Islamic Azad University, Dezful, Iran.*
[3]*Department of Electrical Engineering, Faculty of Engineering, Arak University, Arak, Iran.*
[4]*Research Institute of Renewable Energy, Arak University, Arak, Iran.*

Abstract *— A stochastic multi-objective structure is introduced for integrating hydro-thermal, wind power, photovoltaic (PV), pumped storage hydro (PSH), and large-scale electric vehicle (LS-EV) systems using a day-ahead self-scheduling mechanism. The paper incorporates an improved Harris Hawks Optimizer combined with Particle Swarm Optimization, termed HHO-PSO. Uncertain parameters of the problem, such as energy prices, spinning reserve, non-spinning reserve prices, and renewable output, are also considered. Additionally, the lattice Monte Carlo simulation and roulette wheel mechanism are utilized. By adopting an objective function that optimizes multiple goals, the paper proposes an approach to assist generation companies (GenCos) in maximizing profit (PFM) and minimizing emissions (EMM). However, to make the modeling of the multi/single-objective day-ahead hydro-thermal self-scheduling problem with WP, PV, PSH, and LS-EVs practical, additional factors must be considered in the problem formulation. According to the findings, the HHO-PSO algorithm provides satisfactory values for profit maximization and emission minimization in the day-ahead operation of power systems across all considered cases. The paper applies the proposed method to a 118-bus test network, demonstrating its accuracy and capability.*

Keywords—Self-scheduling unit commitment, uncertainty, HHO-PSO algorithm, PSH and LS-EVs units, modelling.

NOMENCLATURE

Acronyms

BC	Bilateral contract
CMM	Cost minimization
DA-HTSS	Day-ahead hydro-thermal scheduling
DASMO-HTSS	Day-ahead stochastic multi-objective hydro-thermal self-scheduling
EM	Expected emission
EMM	Emission minimization
EP	Expected profit
FMP	Fuzzy mathematical programming
LMCS	Lattice Monte arlo simulation
LS-EVs	Large-scale electric vehicles
M-PC	multi-performance curves
M/S-O-DA-HTSS	Multi/single-objective day-ahead hydro-thermal self-scheduling
MIP	Mixed-integer programming
MO-HHO-PSO	Multi-objective harris hawks optimizer particle swarm optimization algorithm
MOO	multi-objective optimization
PDF	Probability distribution function
PFM	Profit maximization
POZs	prohibited operating zones
PSH	Pumped storage hydro
RERs	Renewable energy resources
RWM	Roulette wheel mechanism
SMO-HTSS	Stochastic multi-objective hydro-thermal self-scheduling
SOO	single-objective optimization
SP	Stochastic programming
SR, NSR	Spinning reserve, non-spinning reserve
VLC	Valve load cost

Binary variables

$\chi_{n,i,t,s}$	1 if the power output of power plant i exceeds block n of VLC effects curve
$\delta_{n,h,t,s}$	1 if the water volume of reservoir exceeds v_n (h)
$\delta_{n,i,t,s}$	1 if block n in fuel cost curve of power plant i is chosen
$I_{d,i,t,s}$	1 if power plant i supplies non-spinning reserve in the case the power plant is off
$I_{h,t,s}$	1 if hydro power plant h is on
$I_{h,t,s}$	On/off status of power plant h
$I_{i,t,s}$	On/off status of power plant i
$Y_{i,t,s}$	1 if power plant i is shut-down
$Z_{i,t,s}$	1 if thermal power plant i is on

Indices

Received: 25 Feb. 2023
Revised: 16 Aug. 2024
Accepted: 08 Sept. 2024
*Corresponding author:
E-mail: behnamfar50@yahoo.com (M.R. Behnamfar)
DOI: 10.22098/joape.2024.12419.1934

This work is licensed under a Creative Commons Attribution-NonCommercial 4.0 International License.
Copyright © 2025 University of Mohaghegh Ardabili.

I_{ev} Electric vehicle fleet
ev Electric vehicles
h Hydro power plant
i Thermal power plant
p Pumped hydro storage
s Scenario
t Time periods, t = 1, 2, . . . , T (h)
u Upstream reservoir
v Photovoltaic power plant
w Wind power plant

Constants

η^{p}_{sh} Efficiency of the pumped hydro storage (p.u)
η Efficiency of wind turbine
π^{sh} Expected price ($/MWh)
ρ^{s}_{sh} Probability of occurrence of a scenario
$C_{1h}, C_{2h}, C_{3h}, C_{4h}, C_{5h}, C_{6h}$ are the generation coefficients of hydro power plant h
N^{E} Number of electric vehicles
N^{sh} Number of similar PSH power plants involved in the pond
p Power output of wind plant (kW)
P_r Rated generation (kW)
p_s Probability of a scenario
p_w Overall power output of wind plant (kW)
SDC_i Shut-down cost of power plant i ($)
SUC_h Start-up cost of power plant h ($)
v_r Rated output speed of wind (m/s)
v_{in} Cut-in speed of wind (m/s)
v_{out} Cut-out speed of wind (m/s)
$W^{p\ sh}$ Penalty factor for power inequality (p.u)
β^{t} Solar irradiance set as 1000 (W/m^2)
$\pi_{b,t}$ Bilateral contract price ($/MWh)
B^{C}_{EV} Battery size of the electric vehicle
$b_{n,h}$ Slope of the volume block n in the reservoir for power plant h ($m^3/s/Hm^3$)
$b_{n,i}$ Slope of block n in the fuel cost curve of power plant i ($/MWh)
d^{p}_{min}, d^{p}_{max} Pumping power boundaries of pumped hydro storage power plants (MW)
$E(p_{u,n-1,i})$ Emission of the $(n_n - 1)^{th}$ upper limit in emission curve of power plant i (lbs)
$EM^{off}_{i,ns}$ Emission of by the switched-off power plant when supplying N-SR (lbs)
E^{max}_{c} Max charging power of electric vehicle
E^{max}_{d} Max discharging power of electric vehicle
$E^{dr,p}_{n,t}$ Driving power of the nth electric vehicle at hour t
$F(p_{u,n-1,i})$ Generation cost of the $(n_n - 1)^{th}$ upper limit in the fuel cost curve of power plant i ($/h)
g^{p}_{max} A boundary on power output of each pumped hydro storage power plant (MW)
$p_{c,h}$ Output power of power plant h (MW)
p^{i}_{t} Generaiton by thermal power plant
$p^{G,h}_{t}$ Generiton by hydro power plant h at hour t
p^{WG}_{t} Real power ouput of wind turbine
$P^{r,gp}_{w}$ Rated generated power by wind power plant w
$p_{b,t}$ Power scale of BC (MW)
$p_{d,n,i}$ Lower boundary of the nth POZs of power plant i (MW)
$p^{ev}_{max,t,s}$ Electrical generatd by electric vehicles at time t and scenario s
$p^{psh}_{max,t,s}$ Electrical generated by PSH at time t and scenario s
$p^{pv}_{max,t,s}$ Photovoltaic system generation at time t and scenario s
$p^{wp}_{max,t,s}$ Wind power system generation at time t, and scenario s
p^{i}_{max} Max generation by thermal power plant i
$p^{G,h}_{max}$ Max power produced by hydro power plant h
$p^{out}_{min,h,n}$ Min generation by power plant h for PC n (MW)
$p^{out}_{min,i}, p^{out}_{max,i}$ Min and Max output power of power plant i (MW)
p^{i}_{min} Min power output by thermal power plant i
$p^{G,h}_{min}$ Min power hydropower plant hour
$p_{nr,s}$ Normalized probability of scenario
$P^{e}_{rp\,o}$ The rated power output from the photovoltaic power plant
$p_{u,n-1,i}$ Upper boundary of the (nn1)th POZs of power plant i (MW)
$p^{g,p}_{w,t}$ Generaiton by wind power plant
$p^{ch}_{l_{ev},t}$ Charging power of electric vehicle
$p^{dis}_{l_{ev},t}$ Discharging power of electric vehicle
$p_{u_n\,n-1\,i}$ Upper boundary of the (nn1)th POZs of power plant i (MW)
$p^{d\ n_n\,i}$ Lower boundary of the nnth POZs of power plant i (MW)
Q^{h}_{t} Water depletion from hydro power plant h at hour t
Q^{h}_{max} Max water depletion from hydro power plant h
$Q^{out}_{min,h}, Q^{out}_{max,h}$ Min and max water depletion from power plant h (H^3/s)
Q^{h}_{min} Min water depletion from hydro power plant h
$RDL^{p}_{i,t,s}, RUL^{p}_{i,t,s}$ Ramp down and ramp up boundaries of power plant i (MW)
RDL^{n}_{i}, RUL^{n}_{i} Ramp down and up boundaries for block n (MW)
R^{c}_{r} Specific irradiance pointset (120 W/m^2)
SUE_i, SDE_i Start up and shut down emission output of power plant i (lbs)
$SUR_i(i_i)$, $SDR_i(i_i)$ Start up ramp and shut down ramp rate boundaries in power plant i (MW/h)
S^{oc}_{ini} Initial state of charge of electric vehicle
S^{oc}_{max} Max limit of state of charge of electric vehicle
S^{oc}_{max} Max state of charge of electric vehicles
S^{oc}_{min} Min state of charge of electric vehicles
S^{oc}_{min} Min limit of state of charge of electric vehicle
$S^{oc}_{n,t}$ State of charge of the nth electric vehicle
$vol_{max,h,n}$ Maximum volume of the reservoir h for PC n (Hm^3)
$vol_{min,h}$ Minimum volume of the reservoir for power plant h (Hm^3)
v^{h}_{t} Amount of storage of reservoir h at hour t
v^{h}_{final} Ultimate storage of reservoir h
v^{h}_{max} Max storage of reservoir h
v^{l}_{min}, v^{l}_{max} Boundaries on the volume of the downstream reservoir (MWh)
v^{u}_{min}, v^{u}_{max} Boundaries on the volume of the upstream reservoir (MWh)
v^{h}_{min} Min storage of reservoir h
v^{h}_{start} Start storage volume of reservoir h
$v^{i}_{t+1,update}$ Velocity of each particle update
vo^{l}, vf^{l} Start and end water volumes of the downstream reservoir (MWh)
vo^{u}, vf^{u} Start and end water volumes of the upstream reservoir (MWh)
A_W Sweep area
$b_{n,h,k}$ Slope of block n in the performance curve (PC) k of power plant h ($MW/m^3/s$)
c_{su}, c_{su} Start up cost and shut down cost of pumping power plants ($)
N_{WG} Number of turbines (wind generators)
p^{ch} Capacity of power plant h (MW)
L Number of PCs
M Number of POZ s
V Wind velocity (m/s)

Variables

b_c Battery capacity of Electric vehicle
P^{pv} Power out put from a photovoltaic
T^{β^t} Number of times
u^{sh} An integer representing the number of power plants in the pumping state scenario, in t_{sh} equal to 0, . . . , N
v^i, u^i Random numbers in the range of [0, 1]
y^{sh}, Z^{sh} An integer representing the number of power plants that are start-up/shut-down in the pumping state scenario, in t_{sh} equal to 0, . . . , N
β^i A constant value equal to 1.5

$\pi_{sp,t,s}, \pi_{sr,t,s}, \pi_{ns,t,s}$ Market prices for energy, SR , N-SR ($/MWh)
$\psi_{n,i,t,s}$ Generation of block n for power plant i in the VLC effects curve (MW)
σ_c, σ_d Ratios of charging and discharging efficiency of electric vehicles
$EX^{ob,f}_{main}$ Main objective function
$E^{s}_{ob\,f}$ Second objective function (predicted emission for individual Pareto optimal solution) (lbs)
E^{n}_{t} Charging/discharging power of the nth electric vehicle at hour t
$F^{cost,f}_{i,t,s}$ Fuel cost of power plant i ($)
$G^{n,i,t,s}_{G}$ Generation of block n of fuel cost curve of power plant i (MW)
$G_{n,i,t,s}$ Generation of block n in the fuel cost curve of power plant i (MW)
I^{h}_{t} Water inflow from reservoir h at hour t
$profit_{s}$ Profit of scenario s
$p^{sp}_{t,s}$ Power for bidding on the spot market (MW)
p^{D}_{t} The amount of demand at hour t
$p^{out}_{h,t,s}$ Generaiton output from power plant h (MW)
$p^{out}_{i,t,s}$ Generation output from power plant i (MW)
$p^{out}_{max,i,t,s}$ Max generaiton output from power plant i (MW)
p^{fts}_{out} Power output of photovoltaic power plant w (MW)
$p^{out}_{w,t,s}$ Generaiton output from wind power plant w (MW)
Q^{h}_{T} Water deplection from hydro power plant h at hour t
$Q^{out}_{n,h,t,s}$ Water depletion from power plant h and block n (m^3/s)
Q^{nhts}_{out} Water discharge of power plant h and block n (m^3/s)
$SUC_{i,t,s}$ Start up cost of power plant i ($)
S^{h}_{t} Water spillage from hydro power plant h at hour t
$SR_{i,t,s}$, $SR_{h,t,s}$ Spinning reserve of a thermal power plant i and hydro power plant h in the spot market (MW)
$VLC_{i,t,s}$ VLC effects of power plant i ($)
$vol_{h,t,s}$ Water volume in the reservoir related to power plant h (Hm^3)
$vol_{h,t,s}$ ater content of the reservoir related to power plant h (Hm^3)
v^{i}_{t} Velocity of each particle
x^{i}_{best}, x^{i}_{gbest}, $x^{i}_{t,p,p}$ Best sulotion for the current solution , global best solution, position of the particle
$N_{d,h,t,s}, N_{u,h,t,s}$ N-SR of power plant h in the spot market, power plant is off or on (MW)
$N_{d,i,t,s}, N_{u,i,t,s}$ N-SR of power plant i in the spot market, power plant is off or on (MW)
$O_i(N^H_t)$ Computational complexity of the initial process
$v^{u\,sh}$, $v^{l\,sh}$ Energy stored in the upper/lower reservoir in scenario, at the end of t_{sh} (s,MWh)
v A vector containing decision variables
c_1,c_2 Best local and global position weight coefficient
$d^{p\,sh}$ Pumping power input of the PSH power plant in scenario, in t_{sh} (s,MW)
$g^{p\,sh}$ Discharge power of the PSH power plant in scenario, in t_{sh} (s,MW)
p_n Number of competing objective functions in the MMP problem
p_n Number of objective functions in the problem
$p_{sp,t,s}$ Bidding power in the spot market (MW)
q^{p} Number of intervals
w_{ic} The interia coefficient
zh Water transport delay from reservoir z to reservoir h

1. INTRODUCTION

1.1. Motivation and incitement

Similar to other engineering fields, optimization has also been applied to solve complex scheduling problems in power system studies, particularly for day-ahead scheduling of hydro-thermal and renewable energy generation units. In Ref. [1], the hydro-thermal scheduling problem is presented as a complex issue. Maximizing profit for generation companies (GenCos) is discussed as one of the objectives in hydro-thermal self-scheduling (HTSS) in Ref. [2]. Various optimization approaches have been utilized to address this type of scheduling, as noted in Ref. [3]. As observed in Ref. [4], GenCos' profits are maximized by solving an objective function that also considers greenhouse gas emissions in Ref. [5], with the goal of minimizing emission levels. The weighted sum method was employed in Ref. [6] to handle interactions between various objective functions. The epsilon-constrained method was used to minimize both emission and operating costs in Ref. [7]. This approach was similarly adopted in Refs. [8, 9], aiming to minimize pollution emissions while maximizing GenCos' profits. Ref. [10] presents a model for energy market pricing, considering the volatility of prices. Literature in Ref. [11] addresses the clearing problem of energy markets using a stochastic framework. Indefinite pricing in energy markets was utilized for the self-scheduling of thermal energy in a stochastic process in Ref. [12]. The fuzzy distance method was applied in Ref. [13] to solve a stochastic scheduling problem, focusing on uncertain carbon dioxide emission trading. Additional literature, such as in Refs. [7–14], provides further details on methods used to solve power system optimization problems. For instance, Ref. [15] considers the effects of variable load conditions. A stochastic multi-objective self-scheduling (SMO-SS) approach involving profit maximization and emission minimization for hydro-thermal units is presented in Ref. [16]. Various dynamic ramping rates (DRR) for HTSS problems are discussed in Ref. [17]. Wind turbines, as a source of green energy, are noted for their low cost and zero emissions in Ref. [18], despite the intermittent nature of their output as discussed in Ref. [19]. The ε-constraint method has been used to solve the Pareto front and provide solutions to multi-objective formulations. The MO-HTWS problem, including renewables like wind and thermal power, is addressed in Refs. [20, 21]. Ref. [22] uses a modified MO-BCO to solve problems with multiple distinct objectives. The non-dominated sorting genetic algorithm (NSGA-II) is applied in Ref. [23] to address errors caused by constraints and boundaries in optimization problems.

1.2. Literature review

According to Ref. [24], introduced and applied the antlion optimization algorithm to solve several optimization problems in the engineernig. This algorithm can be used for optimization purposes in wind turbines in Ref. [25]. In Ref. [26], adopted a method to analyze small-scale hydro generaiton plant using optimization tools. According to Ref. [27], compared the capital cost, repair and maintenance, and operating cost of different hybrid renewable-based systems. In Ref. [28],introcued a modified NSGA-II algorithm to deal with multi-objective optimization of a hydro-solar system. The authors in Ref. [29], discussed a hybrid wind-solar-thermal energy generation system to boost controllability of the system. Power output of renewable-based systems was rised and demand variations was levelized via load-shifting in Ref. [30]. A scheduling and operation of a combination of hydro, thermal, wind, and solar generation was presented in Ref. [31]. According to Ref. [32], discussed various quantities of the stochastic optimization approach, such as time steps, uncertainty modeling, ate of sampling of the data, and more in the case it is applied to renewable generation units. Ref. [33] presents the generic steps of stochastic optimizations in RERs applications, strating from the modelling of the sampling information and uncertainties. Another study establishes a multi-objective model for the coordinated operation of a H-WP-PV power system in Ref. [34]. According to Ref. [35], one aim of multi-objective optimal operation of hybrid (HT, WP, PV) power systems is emission minimization. In Ref. [36] investigates the potential application of PV, WP and diesel energy system with battery storage in the northern region of Bangladesh. In Ref. [37], refers to an MP

Graphical abstract

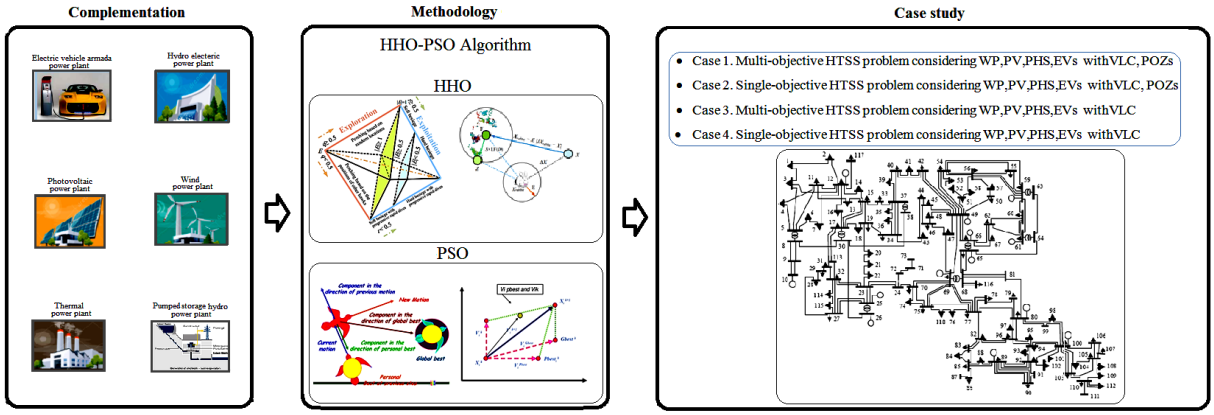

Graphical abstract

technique for the design of off-grid and grid-connected hybrid power systems by taking into account uncertainties in RERs and load demands. According to Ref. [38], focuses on the mixed-integer linear programming for hybrid (WP, Diesel, Battery) power systems with cost and emission minimization (EMM). In Ref. [39], introduces an index, called RER, to represent the energy structure of a country and proposes a u-shaped REKC hypothesis between RER and economic. The authors of in Ref. [40], have addressed the multi-objective model for STHT scheduling problem in the presence of the PSH technology. Renewable microgrid (RMG) has also been discussed in some literature. The authors in Ref. [41], employed an RMG with an EV parking lot to provide controllability on plug-in electrical vehicles (PI-EVs). Also, to find optimal nergy markete strategies, a recent formulation was presented in Ref. [42]. The uncertain parameters (such as the amount of demand, price of energy, pv output, temperature and wind speed) were considered by adopting a hybrid robust stochastic method. Literature, Ref. [43], adopted multi-objective optimization (MOO) to form a hybrid wind, gas turbine, and regenerative electric boiler and find the maximum operating income and minimum operational risk. In Ref. [44] addressed a bidding approach to a WP-T-PV system in energy market. Optimization of the size of a PV, WP, diesel, hybrid microgrid system (HMS) with battery storage (BS) was discussed in Ref. [45], using the multi-objective self-adaptive differential evolution (MOS-ADE) algorithm in the city of yanbu, saudi arabia. An integrated solar-driven co_2 capture system for application in industrial buildings to decarbonize factories' CO_2-rich exhaust gas generated from workers or manufacturing processes, and further conducts multi-objective optimization based on the NSGA-II algorithm. By setting the integrated system's performances, including captured CO_2 mass, net levelized co_2 cost-profit, generated electricity, and exergy efficiency, as the constrained multi-objectives, the effects of system working parameters on them are disentangled and articulated concerning the energy-mass balance principles in Ref. [46]. In Ref. [47] a grid-connected integrated energy systems (IES) is proposed, which considers the complementarity of geo-thermal energy and solar energy and takes heat storage into account. The multi-objective optimization problem of IES is studied for the coupling mode of electric energy, heat energy and cold energy. Taking a multi-functional park as the research object, a multi-objective optimization model was established aiming at integrating operation cost, exergic efficiency and emission gas emission penalty cost. The authors in Ref. [48], A profit-aware recommender system based on swarm intelligence in a multi-objective environment (multi-objective artificial bee colony, MOABC) has been designed, implemented, and applied. According to Ref. [49], focuses on the introduce a compromise programming (CP) framework for solving a multi-objective two-stage stochastic unit commitment problem characterized by high penetration of wind power. The proposed framework aims at finding best-compromise pareto efficient on/off schedules, accounting for wind and power demand uncertainties: such solutions must trade off the three objectives of operating cost, CO_2 emissions, and wind power curtailment in accordance to the decision maker preferences. a two-stage dispatching model for hybrid WP-PV-T power system is established, and the ancillary service market is introduced to coordinate optimization. The first stage model aims at the equilibrium of power generation profits of power producers. Then in the second stage, the equilibrium profits are transformed into constraint, and the day-ahead dispatching model is constructed with the objective of minimizing comprehensive power purchase costs and maximizing renewable energy utilization after considering the balance of economy and social responsibility in Ref. [50]. In Ref. [51], a hydro system with water transport delay among reservoirs is considered here. Optimal utilization of these sources to serve demands over short term of 24h of a day by scheduling their respective generations so as to achieve multi objectives of cost effective production, reduced emission and transmission loss have been studied using a bio-inspired social spider algorithm. According to Ref. [52], focuses on a multi-objective hydro-thermal scheduling (MO-HTS), the hydro and thermal units are arranged to reduce the cost of generation and emission simultaneously. The wind and solar are incorporated with hydro-thermal to get reliable electricity generation at the lowest price with low emission. Whale optimization algorithm (WOA) has been developed as an optimization technique which works on whales' hunting behavior. The authors in Ref. [53], discussed a stochastic structure for generation companies (GenCos) that participate in hydro-thermal self-scheduling (HTSS) with a wind power plant on short-term scheduling for simultaneous reserve energy and energy market. In the proposed framework, mixed-integer non-linear programming of the HTSS problem is converted into a MIP. Since the objective of the study is to show how GenCos aim to achieve profit maximum (PFM), mixed-integer programming is used here. A stochastic single objective framework for GenCos optimal self-scheduling unit commitment under the uncertain condition and in the presence of small hydro (SH) units is proposed. In order to solve this problem, a new meta-heuristic optimization technique named antlion optimizer (ALO) has been used. The objective function of the problem is profit maximization and modeled as a mixed-integer programming problem in Ref. [54]. According to Ref. [55], the main purpose of using this type

of algorithm (Harris Hawks Optimization) is to optimally solve the short-term hydro-thermalself-scheduling (STHTSS) problem with WP, PV, SH and PHS powr plants while considering uncertainties such as energy prices, ancillary services prices, etc, in the energy market.

1.3. Contributions and paper organization

Regarding what has been said and taking a look at Table 1 leads us to point out that one of the highlight of the present rsearch is adoptation of a combined HHO-PSO (considering indefinite parameters like energy, SR and NSR prices, load demand, WP, PV, PSH units, with LS-EVs) for solving the day-ahead M/S-O-HHO-PSO problem. The optimization used in this paper is realized using an MIP. Yet, the paper aims at achieving the PFM and the EM at the same time uncertain quantities and the imposed boundaries related to hydro-thermal, wind, photovoltaic, PSH units, with LS-EVs. So, in the end, we can mentioned the following items as the contributions:

- A genealized mathemtial expression of the stochastic day-ahead multi-objective HTSS (S-DA-MO-HTSS) model with/without WP, PV and PSH units considering VLC, POZs and various types of uncertainties.
- An effective combination of PV, WP, PSH and LS- EVs with HTSS into power system is studied.
- The advantage of the suggested HHO-PSO method is accredit in comaprison to some other algorithms available in the literature.
- A modeling of HTSS is provided in the form of a multi-objective problem with PFM and EMM as two distinctive objectives (F_1, F_2) of MO-HTSS. It then is mathematically expressed and solved considering WP, PV, PSH and LS-EVs.
- Furthermore, as energy price, SR and NSR prices, and WP, PV and load are uncertainties, a PDF was utilized to estimate the values of errors related to these quantities.

The remainder of this paper is as follows. In Section 2, an MIP stochastic multi-formulation including hydro-thermal self-scheduling with WP, PV, PSH units, LS-EVs are provided. In Section 3, stochastic modeling of uncertainties are presented. Section 4 discusses the models of renewable energy system. Sections 5 and 6 describbe the model of pumped-storage hydro-electricity units and model of electrice vehicle, respectively. Sections 7, 8 and 9 introduce and show how (solution methods taking into account the multi-objective optimization) to use HHO, PSO and HHO-PSO algorithms, respectively. In Section 10, an IEEE 118-bus test system has been adopted and validity of the method is approved by testing various cases. Section 11 gives a comparison between the present study and some other literature. in the end, conclusions are reported in Section 12.

2. Problem Formulation

2.1. Objective functions

A) Profit maximization

The first function in the problem of optimization of MO-HTSS that tries to maximize expected profit $EX_{main}^{ob,f}$ and profit is given as follows:

$$f_{\max}^{1} \rightarrow EX_{main}^{ob,f} = \sum_{s\in Ns}\Big[p_{b,t}(\pi_{b,t}) + p_{nr,s}(profit_s) + p_s(p_{\max,t,s}^{psh} + p_{\max,t,s}^{wp} + p_{\max,t,s}^{pv} + p_{\max,t,s}^{ev})(\pi_{b,t})\Big] \quad (1)$$

$$profit_s = \sum_{t\in T}\left\{\begin{array}{l}\pi_{sp,t,s}\ (p_{sp,t,s}) + \sum_{i\in I}\{(SR_{i,t,s})\pi_{sr,t,s} + (N_{u,i,t,s} + N_{d,i,t,s})\ \pi_{ns,t,s}\} \\ + \sum_{h\in H}\{(SR_{h,t,s})\pi_{sr,t,s} + (N_{u,h,t,s} + N_{d,h,t,s})\pi_{ns,t,s}\} - \sum_{h\in H} SUC_h(Z_{i,t,s}) \\ - \sum_{i\in I}\{F_{i,t,s} + SDC_i\ (Y_{i,t,s}) + SUC_{i,t,s} + VLC_{i,t,s}\}\end{array}\right\} \quad (2)$$

$EX_{\text{main}}^{\text{ob,f}}$; There are two terms in the second part of this funciton. The first denotes a bilateral contract used to extract invariant income. Eq. (2) expresses the sum of product of time periods of sceanrios and probability of the related profit.

B) Minimization of emission

As previously mentioned, the second function minimizes the amount of emission produced by non0renewables:

$$f_{\min}^{2} \rightarrow Em_{main}^{ob,f} = \sum_{s\in Ns}(p_{nr,s})\sum_{i\in EGC}\sum_{t\in T}\left\{\begin{array}{l}\sum_{n=1}^{NEM}\left[(G_{n,i,t,s}(ben_{n,i}) + \delta_{n,i,t,s}\,E(p_{u,n-1,i}))\right] \\ + SDE_i\ (Y_{i,t,s}) + SUE_i\ (Z_{i,t,s}) + EM_{i,ns}^{off}(I_{d,i,t,s})\end{array}\right\} \quad (3)$$

Ref. [56], presents different kinds of emission, like SO_2 and NO_x resulting from the operaton of non-renewables. Fig. 1 illustrates the optimization process.

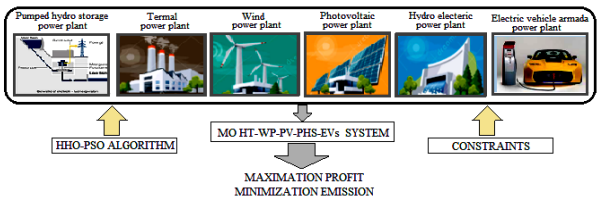

Fig. 1. The proposed multi-objective HHO-PSO optimization framework (for FPM and EMM).

System load balance as one of the important constraints can be expressed by summing up power output of HT/WP/PV/ PSH and LS-EVs units, and this equals the load. This is given in Eq. (4):

$$\sum_{i=1}^{N^I} p_{i,t,s}^{out} + \sum_{h=1}^{N^H} p_{h,t,s}^{out} + \sum_{w=1}^{N^W} p_{w,t,s}^{out} + \sum_{V=1}^{N^V} p_{v,t,s}^{out} + \sum_{P=1}^{N^P} p_{p,t,s}^{out} + \sum_{ev=1}^{N^{ev}} p_{ev,t,s}^{out} - N^E(E_{n,t}^{dr,p}) + (p_{l_{ev,t}}^{dis} - p_{l_{ev,t}}^{ch}) = p_t^D \quad (4)$$

2.2. Model of thermal units

Considering nonlinear formulae of thermal units, the mathematical formulations should be linearized as discussed in subsubsections A) to C).

A) Fuel cost function with POZs

The second-order formulation of fuel cost for a thermal unit is given here. Consideirng the discrete natue of this function, we need to use a linearized model that consists of M POZs. So, the function can be written as:

$$F_{i,t,s}^{\cos t,f} = \sum_{n=1}^{M+1}\left[(G_{n,i,t,s})\,b_{n,i} + (\delta_{n,i,t,s})\,F(p_{u,n-1,i})\right]\ \forall i\in I, \forall t\in T, \forall s\in S \quad (5)$$

Table 1. Contributions and objectives of the literature and present work.

Authors/year	Hybrid system	Objective function	Solution approach
Hetzer *et al.* (2008)	Thermal-wind	CMM	Numeric optimization
Liu and Xu (2010)	Thermal-wind	EMM	Numerical optimization
Mondal *et al.* (2013)	Thermal-wind	CMM and EMM	Gravitational search algorithm
Ismail *et al.* (2013)	Wind-PV-diesel	CMM and EMM	Optimization toolbox
Panda and Tripathy (2014)	Thermal-PV	CMM, reactive power	Modified bacteria foraging algorithm
Mukhtaruddin *et al.* (2015)	Wind-PV-battery	CMM Reliability maximization	Iterative pareto fuzzy technique
Panda and Tripathy (2015)	Thermal-wind	CMM, voltage security enhancement	Modified bacteria foraging algorithm
Panda and Tripathy (2016)	Thermal-wind	CMM, EMM and loss Min	Hybrid algorithm
Abdelaziz *et al.* (2016)	Thermal (3Generator)	CMM and EMM	Flower pollination algorithm
Neto *et al.* (2017)	Hydro-wind-PV	Effective reallocation of energy	Markowitz portfolio theory
Wang *et al.* (2017)	Hydro-wind-PV	Generation maximization	Non dominated sorting genetic algorithm
Biswas *et al.* (2017)	PV-wind	CMM	Adaptive differential evolution
Jurasz and Ciapala (2017)	PV-hydro	Minimization of energy demand variability	Mixed integer mathematical modelling
Panda *et al.* (2017)	Hydro-thermal-wind	CMM, voltage security enhancement	Modified bacteria foraging algorithm
Ramli *et al.* (2018)	PV-wind-diesel	CMM reliability enhancement	Self-adaptive differential evolution
Rahmani *et al.* (2018)	Wind-thermal	CMM reliability enhancement	Self-adaptive differential evolution
Mandal *et al.* (2018)	Wind-PV	CMM and EMM	Homer software
Massrur *et al.* (2018)	Wind-thermal	CMM and computational time minimization	Modified cuckoo search algorithm
Mahmoudimehr *et al.* (2018)	PV-hydro	CMM and loss Min	Genetic algorithm
Movahediyan *et al.* (2018)	PV-diesel	CMM and loss Min	Crow search algorithm
Lee *et al.* (2019)	Wind-PV-battery	CMM and EMM	Chance constrained programming and fuzzy model
Li *et al.* (2020a,b)	Thermal-PV-battery	Fuel consumption, pollution minimization	Chao mutation whale optimization algorithm
Liwei *et al.* (2019)	Wind-Gas turbine-Regenerative Boiler	Revenue maximization, Risk Min	GAMS software with ILOG solver
Rakhshani *et al.* (2019)	Wind,battery,diesel	CMM and EMM	Mixed integer linear programming
Yao *et al.* (2019)	Thermal, PV, wind, hydro	Renewable energy consumption rate,EMM	Renewable energy Kuznets Curve (RKC)
Simab *et al.* (2018)	Hydro-thermal-psh	CMM and EMM	Vikor method
Aliasghari *et al.* (2018)	Microgrid	CMM	GAMS software
Abedinia *et al.* (2019)	Large consumer	CMM	Robust optimization
Ambarish Panda *et al.* (2020)	Hydro, thermal, wind, PV	CMM,EMM and power loss Min	Modified bacteria foraging algorithm and Fuzzy membership Approach
Hooman Khaloie *et al.* (2020)	Wind-thermal-PV	EMM and PFM	Weighted sum method, fuzzy satisfying approach
The present study	Hydro, thermal, wind, PV, psh, EVs	EMM,PFM	HHO-PSO algorithm

$$p^{out}_{i,\,t,\,s} = \sum_{n=1}^{M+1} [G_{n,i,\,t,\,s} + (p_{u,n-1,\,i}\,)(\delta_{n,i,\,t,\,s})]\ \ \forall i \in I, \forall t \in T, \forall s \in S \tag{6}$$

As is seen in Eq. (5), the fuel cost function of thermal units is formed based on binaries. The equation also shows the ramp and power output of block n. Generation by these units is presented in Eq. (6). Linearization of the mentioned function can be realized as in Eqs. (7)-(9) with the related boundaries:

$$G_{n,i,\,t,\,s} \geqslant 0\ ;\ \ n = 1, 2, ..., M+1\ \ \forall i \in I, \forall t \in T, \forall s \in S \tag{7}$$

$$(\delta_{n,i,\,t,\,s})\ [p_{d,n,\,i} - p_{u,n-1,\,i}] \geqslant\ G_{n,i,\,t,\,s}\ \ ;\ \ n = 1, 2, ..., M+1 \tag{8}$$

$$\sum_{n=1}^{M+1} \delta_{n,i,\,t,\,s} = I_{i,\,t,\,s} \tag{9}$$

Eq. (7) assesses the maximum and minimum generaitons, respectively shown by $P_{d,M+1,i=Pmax,i}$ and $P_{u,0,I} = P_{min,i}$ with respect to the upper and lower boundaries.

B) VLC effects

As given in Refs. [15, 16], the VLC effect function is sinusoidal and nonlinear for thermal generation units.

C) Boundaries on the size of thermal units

The following presents the lower and upper limits on the operation of thermal power plants, shown by RDL and RUL:

$$\left[p^{out}_{\min,i}(I_{i,\,t,\,s})\right] \leqslant p^{out}_{i,\,t\,,s} \leqslant \left[p^{out}_{\max,i,\,t,\,s}\right] \tag{10}$$

$$\left[p^{out}_{\max,i,\,t,\,s}\right] \leqslant \left[(Y_{i,\,t+1,\,s})\ SDR_i(i_i)\ + p^{out}_{\max,i}(I_{i\,,t,\,s} - Y_{i\,,t+1\,,\,s})\right] \tag{11}$$

$$\left[p^{out}_{i,\,t-1,\,s} - p^{out}_{i,\,t\,,s}\right] \leqslant \left[SDR_i(i_i)\ (Y_{i,\,t,\,s}) + RDL^{p}_{i\,,t,\,s}\right] \tag{12}$$

$$\left[(RUL^{p}_{i,\,t\,,s}) + SUR_i(i_i)\ (Z_{i,\,t+1\,,s})\right] \geqslant \left[(p^{out}_{i\,,t+1\,,s}) - (p^{out}_{i,\,t\,,s})\right] \tag{13}$$

D) Dynamic RDL and RUL

As per in Ref. [17], for ∀i ∈ I, ∀t ∈ T, ∀s ∈ S and considering the data obtained in the previous sections, there are upper and lower boundaries on the operation of thermal geneation units. Eqs. (14) and (15) determine the dynamic RDL and RUL concering the operation of plants:

$$RDL^{P}_{i,t,s} = \sum_{n=1}^{M+1} (\delta_{n,i,\,t\,,s})\ RDL^{n}_{i}\ \ \forall i \in I, \forall t \in T, \forall s \in S \tag{14}$$

$$RUL^{P}_{i,t,s} = \sum_{n=1}^{M+1} (\delta_{n,i,\,t\,,s})\ RUL^{n}_{i}\ \ \forall i \in I, \forall t \in T, \forall s \in S \tag{15}$$

E) Several other constraints on thermal units

Ref. [57], presents the SR and NSR as reserve services, which respectively are related to active and reactive power. Also, as is stated in Ref. [2], the startup cost function, MUT, MDT, and some other quantities are the rest of limits concering the thermanl unit. The constraints on unit commitment and scheduling of thermal units, as well as the limits on the rate of discharge of the units can be found in Ref. [57]. The last constraint, i.e. the rate of discharge is presented as follows:

$$P^{i}_{\max} P^{i}_{t} P^{i}_{\min} \tag{16}$$

2.3. Model of hydro units

Subsections A), B) and C) provide the related limits on the operaiton of hydro power generation units.

A) Linearized expressions of volume and multi-performance curves

The following equations present linearized equalities and inequalities concerning the performance curves of hydro power plants. These are specified accoridng to the amount of water within the reservoires:

$$vol_{h,\,t,\,s} \geqslant v_{\max,h,\,n}\ ;\ \forall h \in H \tag{17}$$

$$\delta_{L-1,h,\,t,\,s}(vol_{\max,h,\,L}) + \sum_{n=2}^{L} [\delta_{n-2,h,\,t,\,s} - \delta_{n-1,h,\,t,\,s}](vol_{\max,h,\,n-1}) \geqslant vol_{h,\,t,\,s} \tag{18}$$

$$vol_{h,\,t,\,s} \geqslant \delta_{L-1,h,\,t,\,s}(vol_{\max,h,\,L-1}) + \sum_{n=3}^{L} [\delta_{n-2,h,\,t,\,s} - \delta_{n-1,h,\,t,\,s}](vol_{\max,h,\,n-2}) \tag{19}$$

$$\delta_{L-1,h,\,t\,,s} \leqslant \ldots \leqslant \delta_{2,h,\,t,\,s} \leqslant \delta_{1,h,\,t\,,s} \tag{20}$$

B) Linear power discharge performance curves

This model describes two stages. One deals with water depletion from the reservoirs and the produced water. The other includes performance curves (L). Thus, linearized form of formulations can be presented as follows:

$$\left[p^{out}_{h,\,t,\,s} - p^{out}_{\min,h,k}(I_{h,\,t,\,s})\right] - \sum_{n\in N}\left[Q^{out}_{n,h,t,s}\,(b_{n,h,\,k})\right] - [(k-1) - \sum_{n=1}^{k-1}(\delta_{n,h,\,t,\,s}) + \sum_{n=k}^{L-1}(\delta_{n,h,\,t,\,s})](p_{c,h}) \leqslant 0\ ;\ 1 \leqslant k \leqslant L \tag{21}$$

$$\left[p^{out}_{h,\,t,\,s} - p^{out}_{\min,h,k}(I_{h,\,t,\,s})\right] - \sum_{n\in N}\left[Q^{out}_{n,h,t,s}\,(b_{n,h,\,k})\right] + [(k-1) - \sum_{n=1}^{k-1}(\delta_{n,h,\,t,\,s}) + \sum_{n=k}^{L-1}(\delta_{n,h,\,t,\,s})](p_{c,h}) \geqslant 0\ ;\ 1 \leqslant k \leqslant L \tag{22}$$

C) Several other constraints on hydro units

The following provides the rest of limits and boundaries on the operaiton of hyrdo generation units. These include, but not limited to, water depletion from rservoirs.

C).1. Generation limits

$$p^{G,m}_{\max} \leqslant p^{G,m}_{t} \leqslant p^{G,m}_{\min} \tag{23}$$

The relationship between hydro power generation, water deplection rate and the reservoir capacity can be written as:

$$p^{G,h}_{t} = c_{1h}\,(v^{h}_{t})^2 + c_{2h}\,(Q^{h}_{t})^2 + c_{3h}(v^{h}_{t})(Q^{h}_{t}) + c_{4h}\,(v^{h}_{t}) + c_{5h}\,(Q^{h}_{t}) + c_{6h} \tag{24}$$

C).2. Start and final resrvoir storage volumes limits

$$v^{h}_{start} = v^{h}_{0}\ , v^{h}_{final} = v^{h}_{T} \tag{25}$$

C).3. Water dynamic balance limits

$$v^{h}_{t} = \sum_{z=1}^{N^z}[(S^{z}_{t-\tau_{zh}}) + (Q^{z}_{t-\tau_{zh}})] + v^{h}_{t-1} - Q^{h}_{T} - S^{h}_{t} + I^{h}_{t} \tag{26}$$

C).4. Reservoir volume limits

$$v^{h}_{\min} \leqslant v^{h}_{t} \leqslant v^{h}_{\max} \tag{27}$$

C).5. Water discharge rate limits

$$Q^{h}_{\min} \leqslant Q^{h}_{t} \leqslant Q^{h}_{\max} \tag{28}$$

3. STOCHASTIC MODELING OF UNCERTAINTIES

Uncertainty in power systems is of critical importance. It includes the uncertain nature of demand prediction error or unexpected outage of power system devices (e.g. generation units and transmission lines). Ref. [45], used LMCS as a method of simulation of outage of different power generation units. Also, considering the error in predicting energy price, we can adopt some other uncertain parameters (WP/PV/load) that are somehow in relation with energy price. Standard deviation of price prediciton error (σ) was given in Refs. [58, 59]. The RWM was adopted [59, 60] to generate price scenarios for time periods concerning different predicitons and probability values of the PDF. As the number of produced scenarios is considerable, we need a method to reduce it, in which scenarios that are less probable to happen are discarded in Refs. [58, 59], and those more probable scenarios are kept to be used in the ST-MOHTSS problem with WP/PV/PSH generation units.

3.1. Load uncertainty modeling

Load uncertainty is assumed as load prediction error in this part of the paper. Therefore, the performance of the load probability distribution due to the prediction error should be based on past information about the loads. Inclusion of all seprate loads as a variable will certainly crwod the problem and make its solution more complicated. So, the demand can be treated here in the form of a random variable. And, the distance between levels of load prediction error equals the standard deviation of the error. But, it is essential to proper model for the random load level as a random variable. RWM has been used to realize this in Ref. [61]. First, as the sum of probabilities must be 1, the probability of varying levels of load prediction error have to be applied to a unit load. Then, the probability of load prediction error is covered by normalization between [0, 1]. However, the higher the probability of load prediction error, the more space the RWM will occupy. After the RWM is formed, random numbers are produced between [0, 1]. The generated numbers are placed in the desired ranges on the RWM with different levels of load prediction error. Therefore, RWM helps model random load behavior to generate new scenarios. For better modeling, more scenarios are needed, but the presence of uncertainty will increase the computation time. It should be noted that some scenarios, after producing different scenarios, may be very unlikely, which can increase the computation time. So, it is necessary to remove the scenarios with small values in Ref. [60].

4. MODELING RENEWABLE ENERGY SYSTEM

4.1. Modeling wind turbines

The dependency of power produced by a wind turbine to the wind speed was modeled in Refs. [21, 22]. To deal with HTSS problems, the intermittent nature of wind need to be considered. Weibull probability density in Ref. [22], can be adopted to explain the behavior of wind velocity and PDF will be obtained as Eq. (29). Parameters of the function are c > 0 and k > 0:

$$pdf_{k,\,c}^{\nu} = \left(\frac{k_i}{c}\right)\left[\left(\frac{\nu}{c}\right)^{k_i-1}.e^{(-(\frac{\nu}{c})^{k_i})}\right] \qquad (\nu > 0) \tag{29}$$

In this equation, v is the wind velocity. As per the pdf of this parameter, the cdf will be expressed as:

$$cdf_{k,c}^{\nu} = 1 - (e^{(-(\frac{\nu}{c})^{k})}) \tag{30}$$

Eq. (31) shows how much a wind turbine can produce power depending on wind velocity:

$$P = \begin{Bmatrix} 0 & v \leqslant v_{ci} \\ (a + bv + cv^2) & v_r \geqslant v \geqslant v_{ci} \\ p_r & v_{co} \geqslant v \geqslant v_r \\ 0 & v \geqslant v_{co} \end{Bmatrix} \tag{31}$$

Parameters of functions v_{ci} and v_r for a, b and c are found based on the following relationships:

$$a = \frac{1}{(v_{ci} - v_r)^2}((v_r + v_{ci})\, v_{ci} - (\frac{v_{ci} + v_r}{2v_r})^3 4\, v_{ci} \times v_r)$$

$$b = \frac{1}{(v_{ci} - v_r)^2}((\frac{v_{ci} + v_r}{2v_r})^3 \times 4(v_{ci} + v_r)\, v_{ci} - 3(v_{ci} + v_r))$$

$$c = \frac{1}{(v_{ci} - v_r)^2}(2 - 4(\frac{v_{ci} + v_r}{2v_r})^3)$$

Eq. (32) calculates the pdf by assuming that wind speed varies between $[v_{in},\, v_r]$:

$$pdf_{w}^{w} = (\frac{kh}{w_r})(\frac{\nu_{in}}{c})\left[(1 + \frac{hw}{w_r})(\frac{\nu_{in}}{c})\right]^{k-1}.\exp\left\{-\left[(1 + \frac{hw}{w_r})(\frac{\nu_{in}}{c})\right]^{k}\right\} \tag{32}$$

Since $h = (v_r/v_{in}) - 1$, Eq. (26) has ben adopted for continuous probabilities. The *cdf* of parameter w will be:

$$cdf_{w}^{w} = \begin{Bmatrix} 0 & (0 > w) \\ (\frac{\nu_{in}}{c})(\frac{kh}{w_r})\left[\frac{\nu_{in}}{c}(1 + \frac{hw}{w_r})\right]^{k-1}.\exp\left\{-\left[(\frac{\nu_{in}}{c})(1 + \frac{hw}{w_r})\right]^{k}\right\} & (w_r > w \geqslant 0) \\ 1 & (w_r \leqslant w) \end{Bmatrix} \tag{33}$$

The toal amount of power generation by wind turbines placed across the network can be calculated based on Eq. (34):

$$p_t^{WG} = p_W.\, A_W.\eta.\, N_{WG} \tag{34}$$

Where A_W is the total area occupied by wind turbine generation units, η shows the efficiency of wind system inverter and N_{WG} expresses the number of critical generation units related to wind systems.

A) Wind plant power generation limits

$$p_{w,t}^{g,p} \geqslant P_w^{r,gp} \geqslant 0 \tag{35}$$

4.2. Modeling photovoltaics

The amount of power generation by PV arrays can be found from:

$$P_{\beta_t}^{pv} = \begin{Bmatrix} P_{rp\,o}^{e}\left(\frac{{\beta_t}^2}{R_r^c.\beta_{rs}^s}\right) & R_r^c > \beta_t > 0 \\ P_{rp\,o}^{e}\left(\frac{\beta_t}{\beta_{rs}^s}\right) & \beta_t > R_r^c \end{Bmatrix},\ t = 1, ...T \tag{36}$$

5. Model of Pumped Storage Hydroelectricity Units

In Ref. [62], the PSH power plant consists of two upstream and downstream sources with pumps reversible turbines that can operate in either generator or motor modes. The PSH unit pumps water to the upstream source during peak network consumption with power consumption, and at peak consumption times, water is transferred from the upstream source to the downstream source by generating electrical energy. in this case, the water turbine operates in generator mode. This cycle is economically viable because at non-peak times the electricity is inexpensive and at times of peak consumption the electricity is cheap so that income gained from selling energy offsets the cost of buying energy and system losses. The volume of water behind the upstream and downstream sources is considered energy. The mathematical model of the PSH units in operation is given in Eq. (37):

$$\text{subject to } \nu^{u\,sh} = \nu^{u\,sh-1} + \eta_{sh}^{p}(d^{p\,sh}) - g^{p\,sh}\ \forall s \in S, \forall t \in T \tag{37}$$

$$subject\ to\ \nu^{u\,sh} = \nu^{u\,sh-1} + \eta_{sh}^{p}(d^{p\,sh}) - g^{p\,sh}\ \forall s \in S, \forall t \in T \tag{38}$$

$$\nu_{\min}^{u} \leqslant \nu^{u\,sh} \leqslant \nu_{\max}^{u}\ \ \forall s \in S, \forall t \in T \tag{39}$$

$$\nu_{\min}^{u} \leqslant \nu^{u\,sh} \leqslant \nu_{\max}^{u}\ \ \forall s \in S, \forall t \in T \tag{40}$$

$$\nu_{\min}^{l} \leqslant \nu^{l\,sh} \leqslant \nu_{\max}^{l}\ \ \forall s \in S, \forall t \in T \tag{41}$$

$$\nu^{u\,sh} = \nu f^{u},\ \nu^{l\,sh} = \nu f^{l}\ \ \forall s \in S, \forall t \in T \tag{42}$$

$$u^{sh+1} = u^{sh} + y^{sh} - z^{sh}\ \ \forall s \in S, \forall t \in T \tag{43}$$

$$d_{\min}^{p}(u^{sh}) \leqslant d^{p\,sh} \leqslant d_{\max}^{p}(u^{sh})\ \ \forall s \in S, \forall t \in T \tag{44}$$

$$\left\{(1 - \frac{1}{N}).u^{sh}\right\} \geqslant t^{sh},\ t^{sh} \in \{0, 1\}\ \ \forall s \in S, \forall t \in T \tag{45}$$

$$N(g_{\max}^{p}) \geqslant x_h^{p} \geqslant N(-d_{\min}^{p})\ \ \forall s \in S, \forall t \in T \tag{46}$$

$$u^{sh}, y^{sh}, z^{sh}\ \in \{0, 1, ..., N\}\ \ \forall s \in S, \forall t \in T \tag{47}$$

$$N(t^{sh})(g_{\min}^{p}) \geqslant g_{sh}^{p} \geqslant 0\ \ \forall s \in S, \forall t \in T \tag{48}$$

In these relationships, the output variables $g^{p\ sh}$ and $d^{p\ sh}$ are the consumption variables of the storage pump power plant, and z^{sh} and y^{sh} are the on and off units in each scenario and hour, respectively. The variable x^{ph} is proposed to produce a PSH power plant per hour. The variable v shows the volume of source energy in each of the upstream and downstream sources. The maximum volume $v^u_{\max}$, $v^u_{\max}$ and $v^I_{\min}$, $v^u_{\min}$ of the resource capacity are considered 0 MW and 80 MW, respectively. The size of the two sources is assumed to be equal:

$$(g^p_{\max}.(N) + g^w_{\max}) \geqslant x^{wp\,h} \geqslant -(d^p_{\min}.(N)) \quad \forall s \in S, \forall t \in T \tag{49}$$

The efficiency of the PSH unit system is %80. Eq. (37) with constraints Eqs. (38) to (47) show the objective function of the PSH power plant. The first sentence refers to the revenue earned from energy sell, the second and third sentences denote the cost imposed on the unit due to switching on and off, respectively. The fourth sentence shows the cost of an imbalance in energy production or consumption. The remaining energy when operation is terminated can be found from Eq. (42). It assumed that for $T = 1$, $v^{l\ sh-1}$ equals vo^l and $v^{u\ sh-1}$ equals vo^u. Variable u^{sh} shows the number of pump-turbine units operating in a given hour. For each reservoir, the water balance Eqs. (38) and (39) must be satisfied. Eq. (43) shows how these to parameters are interrelated. Eq. (46) states the dependency of amount of energy market biddings to the mentioned capacities.

6. Model of Electric Vehicle

As we know, electric vehicles (EVs) may take the role of a load or a power supply. Therefore, in intelligent planning, EVs are a assumed as flexible resources for specific strategies. EVs are used as a power supply in a power system during peak loads. During the off-peak hours, EVs can be adopted as electrical demand. When using EVs, the main curve of electricity demand will decrease, taking into account the emission by thermal units, and will follow an increasing trend by considering profit along with other production units. Regarding the operation and cooperation of large-scale EVs, it is necessary to pay attention to planning based on energy prices and output power in 24 hours. in this article, a large scale of EVs have been used for simplicity and uniform performance of fleet EV in Ref. [63]. In fleet mode operation of EVs, the total operating time includes (i) driving, (ii) charging and (iii) discharging windows. Driving windows can be considered to be time intervals from 6-9 a.m. and 4-7 p.m. for EVs operation. If necessary, the window can be charged or discharging window from 19-24 pm. As a result, we can use Eq. (50) to express the charge and discharge power for a fleet of EVs. The value of each EV can be obtained from Eq. (50).

$$\left\{ \begin{array}{l} p^{ch}_{lev,t} = -\sum_{n=1}^{N^e} Min(0, E^n_t) \\ p^{dis}_{lev,t} = \sum_{n=1}^{N^e} Max(0, E^n_t) \end{array} \right\} \tag{50}$$

$$S^{oc}_{n,t} = S^{oc}_{n,t,ini} - \left\{ (\frac{1}{b_c}) \sum_{k=1}^{t} [\min(0, E^n_k) \cdot \sigma_c] + \max(0, E^n_k) \cdot \sigma_d + E^{dr,p}_{n,t} \right\} \tag{51}$$

If $S^{oc}_{n,t} = S^{oc}_{\max}$, E^n_t will be defined as Eq. (52):

$$E^n_t = \left[\frac{B^C_{EV}}{\sigma_c} \right] (S^{oc}_{n,t-1} - S^{oc}_{n,t}) \tag{52}$$

If $S^{oc}_{n,t} = S^{oc}_{\min}$, E^n_t will be defined as Eq. (53):

$$E^n_t = \left[\frac{B^C_{EV}}{\sigma_d} \right] (S^{oc}_{n,t-1} - S^{oc}_{n,t}) \tag{53}$$

The estimated power to drive an EV is 0.75kW, which leads us to conclude that the amount of energy for the EV fleet would be 180 MWh (40,000×0.75×6 kWh) in one day. Hence, energy is wasted when EVs are used as flexible resources; the reason is that the ratio of charging to discharging efficiency is smaller than unity.

6.1. Operation limits on EVs

A) Limits on charging and discharging power

$$\begin{array}{l} 0 > E^n_t \geqslant -E^{\max}_c \text{ for charging} \\ 0 < E^n_t \leqslant -E^{\max}_d \text{ for discharging} \\ E^n_t = 0 \quad \text{for driving} \end{array} \tag{54}$$

B) Limits on state of charge of EV

$$S^{oc}_{\max} \geqslant S^{oc}_{n,t} \geqslant S^{oc}_{\min} \tag{55}$$

C) Limits onc harging and discharging power

$$S^{oc}_{ini} \geqslant S^{oc}_{n,T} \geqslant S^{oc}_{n,0} \tag{56}$$

7. Harris Hawks Optimization Algorithm

Harris hawks algorithm can display a variety of chase styles and bait escape patterns. Displacement happens as the best hawk (the leader) dives into the prey but fails to catch the prey, at which point the prey is chased by another hawk. This way of moving can be seen in different situations. This method of activity is very important to confuse the escaping prey. The most important advantage of this method is the cooperation of harris hawks in identifying the prey, which can cause wear and tear and increase its vulnerability. In addition, as the prey is confused, its defenses are taken away, and ultimately, it cannot escape the siege of the hawks because the most potent and experienced hawk is the tired prey in Ref. [64]. It surrenders and shares its experience with other members of the group. The HHO algorithm solves the problem based on steps decsribed in subsections 7.1-7.9. Fig. 2 shows all the steps of the HHO algorithm.

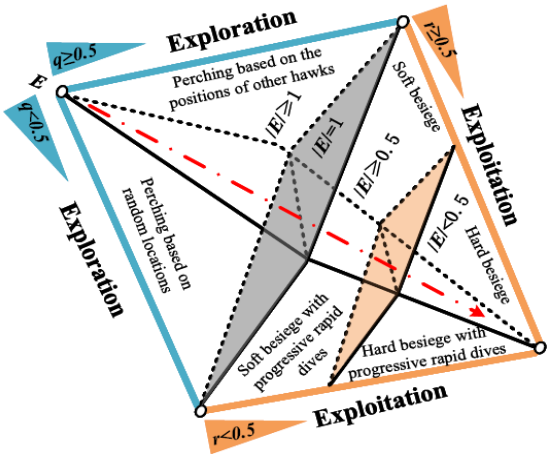

Fig. 2. Different phases of HHO.

7.1. Exploration phase

The exploration phase is described here. Due to the innate features of the harris hawk, it is able to detect, track and hunt prey with its powerful eyes, but sometimes fails to see the prey easily. So, the hawk waits and carefully observes the surroundings to recognize a prey. In this algorithm, hawks are randomly placed in different areas and wait until they may identify the prey following two strategies (the same chances are asssumed for each of the strategies). Strategy (i): The hawks specify their position according to that of other hawks and the location of the prey, which depends on the strategy of being sufficiently close to them when attacking). In Eq. (57), for $0.5 > q_i$, the formula is obtained. Strategy (ii): The hawks are randomly placed on long random places (on tall trees) that are modeled in Eq. (57) subject to $\mathrm{q_i} \geqslant 0.5$.

$$X^{t+1} = \begin{Bmatrix} X_t^{rand} - r^1 \left| X_t^{rand} - 2r^2 X^{t+1} \right| & q_i \geqslant 0.5 \\ (X_t^{rabbit} - X_t^m) - r^3 \left(L^B + r^4 \left(u^B - L^B \right) \right) & q_i < 0.5 \end{Bmatrix} \quad (57)$$

In modeling random of places production between L^B and U^B, two laws must be considered; First law: in this law, solutions are produced based on random locations as well as other hawks. The second law: In Eq. (57), a random component according to the range of variables should be taken into account in addition to the distinction between the best and average position of hawks. In this law, we can add a longitudinal scale to L^B to a random motion. Also, a random scale factor can be considered for the component so that more different steps are provided and distinctive areas of the desired domain are discovedred. Eq. (58) calculates the average location of all hawks:

$$X_t^m = \left(\frac{1}{N_t^H} \right) \sum_{i=1}^{N_t^H} X_i^t \quad (58)$$

7.2. Moving from exploration to exploitation

Harris hawk algorithm has the capability to be transferred from the exploration phase to the exploitation phase and, among various exploitation trends, it can select the prey according to the remaining energy. The preys' escape energy will decrease over time. Eq. (59) is used to model this:

$$E_F = 2E_i \left(1 - \frac{t}{T} \right) \quad (59)$$

7.3. Exploitation phase

Based on hawk tracking strategies and bait escape behaviors, the Harris hawk algorithm suggests four strategies to complete the process. Preys are always trying to avoid threatening positions. The prey can be assumed to be in a state of successful escape ($r < 0.5$) or unsuccessful escape ($0.5 \leqslant r$), where r shows the chance of prey before the sudden attack of the hawk. When the prey is escaping, the hawks use a hard or soft siege to attack it. In real life, hawks approach their prey with increasing proximity in an effort to increase the likelihood that they will capture and kill the prey through a surprise attack. But, after some time, they lose their energy gradually, after which the continuation of the siege is boosted by the hawks and the prey gets tired and gives up. The soft siege occurs when $|\mathrm{E_F}| \geqslant 0.5$ and the hard siege is formed when $|\mathrm{E_F}| < 0.5$.

7.4. Soft besiege

The prey has enough energy when conditions $|\mathrm{E_F}| \geqslant 0.5$ and $0.5 \leqslant r$ are established, so it is tempting to try to escape with deceptive jumps, but in the end it will not work. During this effort, the hawks will make a surprise attack. They run softly and surround the prey. During this time, the prey also gets more tired. The soft siege is modeled according to Eq. (61):

$$\Delta X^t = X_t^{\text{rabbit}} - X^t \quad (60)$$

$$\Delta X^{t+1} = X_t^{\text{rabbit}} - \Delta X^t - E \left| J_P \left(X_t^{\text{rabbit}} \right) - X^t \right| \quad (61)$$

7.5. Hard besiege

When conditions $0.5 \leqslant r$ and $|\mathrm{E_F}| < 0.5$ are established, the energy is reduced because the prey is sufficiently tired. Furthermore, hawks dangerously encircle their prey by a surprise attack, thereby its formula will be calculated according to Eq. (62):

$$X^{t+1} = X_t^{\text{rabbit}} - E_F \left| \Delta X^t \right| \quad (62)$$

7.6. Soft besiege with progressive rapid dives

In the case conditions $|\mathrm{E_F}| \geqslant 0.5$ and $r < 0.5$ hold, the prey can successfully escape, but the soft siege still remains. This process is smarter than before. In this case, the bait's escape patterns and mutant movements are used to model mathematics, the concept of levy flight or L^F. To elucidate on, hawks make several quick group laps encompass the prey and attempt to gradually modify their location and path due to the preys deceitful movements. In addition, L^F-based patterns have been identified in animal tracking activities such as monkeys and sharks. The result is that L^F-based motion algorithms are used at this stage of the algorithm. Inspired by the behavior of hawks, it can be concluded that when hawks want to hunt a prey in competitive conditions, they gradually choose the best position to attack the prey. Hence, to do a soft siege, the hawks are assumed to decide on their upcoming move as per Eq. (63):

$$Y^i = X_t^{rabbit} - E_F \left| J_P(X_t^{rabbit}) - X^t \right| \quad (63)$$

Next, to determine whther their previous dive was a successful dive, they then compare the potential outcomes of such a move with it. The hawks are thought to dive using the following rule (Eqs. (64)-(66)) based on L^F-based patterns.

$$Q_{i,t}^{CAP} = \left\{ \frac{(K1_{i,t} + K2_{i,t} + K3_{i,t})}{N_s} \right\} \times S_{max}^{CAP} \quad (64)$$

$$\sigma^i = \left[\frac{\Gamma\left(1 + \beta^i\right) \times \sin\left(\frac{\pi\beta^i}{2}\right)}{\Gamma\left(1 + \frac{\pi\beta^i}{2}\right) \times \beta^i \times 2^{\left(\frac{\beta^i - 1}{2}\right)}} \right]^{\frac{1}{\beta^i}} \quad (65)$$

$$LF_x = 0.01 \left[\frac{(u^i \times \sigma^i)}{|V^i|^{\frac{1}{\beta^i}}} \right] \quad (66)$$

Therefore, it is in the phase of soft siege that the last strategy of updating hawks locations can be done by Eq. (67):

$$X^{t+1} = \begin{Bmatrix} Y^i & \text{if } F(Y^i) < F(X^t) \\ Z^i & \text{if } F(Z^i) < F(X^t) \end{Bmatrix} \quad (67)$$

7.7. Hard besiege with progressive rapid dives

When $|E_F| < 0.5$ and $r < 0.5$ are considered, the prey cannot run away because it does not have enough energy. At this point, before the hawks suddenly attack the prey to hunt and kill it, a severe siege ensues. The position of the hard siege is similar to that of the soft siege on the bait side, yet the hawks try to decrease the distance between the escaping prey and its place. As a result, for a severe siege, Eq. (68) is used:

$$X^{t+1} = \begin{cases} Y^i & \text{if } F(Y^i) < F(X^t) \\ Z^i & \text{if } F(Z^i) < F(X^t) \end{cases} \quad (68)$$

Where Y^i and Z^i are calculated from Eqs. (63)-(64) and in Eq. (63) can be found from Eq. (58).

7.8. Computational complexity in harris hawks optimization algorithm

The following three main processes determine how complex the Harris Hawk Optimization (HHO) algorithm is when computing: (i) initialization, (ii) competency assessment, and (iii) updating the hawks. The calculation of the complexity of this mechanism is based on the update, which consists of discovering the best location as well as updating the position of all hawks. So, the computational burden of this algorithm is obtained from Eq. (69):

$$C_c = O_i\left(N_t^H \times \left(\bar{T} + \bar{T}D^P + 1\right)\right) \quad (69)$$

7.9. Pseudocode of HHO

Inputs: The population size N and the maximum iterations t_t
Outputs: Prey's position and its fitness value
Set the random population X_i (i = 1, 2, . . . ,N)
while (termination criterion is not satisfied) **do**
  Compute the fitness values of hawks
  Assume X^{rabbit} as the prey's position (best location)
for (individual hawks (X_i)) **do**
  Update the initial energy E_i and jump strength J_p
  Update E_F as per Eq. (59)
If ($|E_F| \geq 1$) **then** ➲ Exploration phase
  Update the location vector as per Eq. (57)
If ($|E_F| < 1$) **then** ➲ Exploitation phase
If ($r \geq 0.5$ and $|E_F| \geq 0.5$) **then** ➲ Soft besiege
  Update the location vector according to Eq. (61)
Else if ($r \geq 0.5$ and $|E_F| < 0.5$) **then** ➲ Hard besiege
  Update the location vector using Eq. (63)
Else if ($r < 0.5$ and $|E_F| \geq 0.5$) **then** ➲ Soft besiege with progressive rapid dives
  Update the location vector according to Eq. (67)
Else if ($r < 0.5$ and $|E_F| < 0.5$) **then** ➲ Hard besiege with progressive rapid dives
  Update the location vector based on Eq. (68)
Return X^{rabbit}

Steps of the HHO algorithm 7.9.

8. Particle swarm optimization (PSO) algorithm

The particle swarm optimization (PSO) algorithm imitates some animal like birds or fish and is based on population. The solutions found by this algorithm depend on important factors such as the speed, position, fitness value of individual particles and the desirable solution. The velocity of each particle (v_t^i) will also be obtained using Eq. (70):

$$v_{t+1,update}^i = w_{ic} \times v_t^i + c_1 \times rand(x_{best}^i - x_{t,p,p}^i) + c_2 \times rand(x_{gbest}^i - x_{t,p,p}^i) \quad (70)$$

But updating, the position of the particle ($x_{t+1,p,p}^i$) will be achieved using Eq. (71):

$$x_{t+1,p,p}^i = x_{t,p,p}^i + v_1 \times (t+1) \quad (71)$$

8.1. Pseudocode of the PSO

The following is the pseudocode of the PSO:
Inputs: Randomly produce an initial population with a size of N and PSO parameters (v_1, c_1, c_2 and w_{ic}).
Outputs: The best solution ($X_{b,s}$).
Calculate the fittness values of particles.
Find the global best solution ($X_{gb,s}$) and the personal best solution ($X_{b,s}$).
Update the speed and position of solutions based on Eqs. (70) and (71).
Until (Termination criteria are met).

9. HHO-PSO optimization algorithm method

In Ref. [65], a new approach to find solutions to the RES-DGs planning optimization problem is proposed by adopting an improved HHO and PSO. Here, to enhance the efficiency of HHO, a hybrid algorithm called HHO-PSO is incorporated to solve the multi-objective day-ahead self-scheduling (MO-DA-SS) optimization. The HHO algorithm has the ability to use the search space. In additio, the exploration performance of this algorithm needs to be further improved. Therefore, the use of PSO to accelerate and improve its exploration performance has been suggested. Thus, the HHO-PSO algorithm can be used to optimally solve the day-ahead self-scheduling (DA-SS) problem of various units because it has a high convergence speed .In this algorithm, the population of chromosomes and candidate solvers is shown with N and X. Each chromosome has properties that are accompanied by mutations, changes that can be binary encoded from strings of 0 and 1. Here, we can refer to the use of real and decimal encryption. To optimize day-ahead self-scheduling units, it is necessary to encrypt the information needed to optimize the amounts profit and emission production units in the chromosome genes. Nonetheless, the suggested chromosome structure is made up of three parts. The first part involves considering the types of power plant units in the 118-bus power system that need to be determined. The second part is related to genes that show the generation power of different units based on the instantaneous price (24 hours) of energy. In addition, genes have real values between zero and the capacity of HT, WP, PV, EVs and PSH. But, the third part is about the chromosome, the actual values from 0 to 1 are obtained by each gene and show the optimized values for the profit and the emission. However, the amount of genes will always be 1 when the generation units are renewable (WP, PV). It should be noted that the number of genes is assumed identical to the maximum number of generation units. This algorithm first considers the primary values of the solutions. Next, it calculates the fitness values of individual solutions by following Eqs. (2) and (4). In the next step, the best solution, which is the one (X_b) with the smallest fitness value (F_b), is determined. It is then possible to update the rest of solutions using this value and the PSO and HHO functions. The procedure is perfomed by calculating the probability of candidate solutions (X_i) and considering their fitness value in such a way that if the probability (p_i^{rob}) is greater than or equal to

0.5 the operators of the HHO algorithm are used; otherwise, to update the solutions. The present candidate uses the PSO algorithm operators. The solutions upldating task is done until the final stages are reached and the stop conditions are obtained. In such a way that it reaches either the maximum number of population or the satisfactory value of the fitness function is achieved using Eq. (72).

$$x^{i}_{t+1,p,p} = x^{i}_{t,p,p} + v_1 \times (t+1) \tag{72}$$

9.1. Incorporation of the HHO-PSO algorithm

Several step must be taken before applying the HHO-PSO algorithm to the optimization problem:

Step 1: Input the information of the power system (including model parameters and initial prediction of electricity price, HT,WP, PV, PSH and LS-EVs powers).

Step 2: Adopt the RWM and LMCS for random scenario production. Also, the PDF is used to predict their errors (WP, PV power, price energy, reserve SR and NSR prices, load).

Step 3: Define (i) parameters of HHO-PSO, (ii) control variable and their limits, and (iii) objective functions to be optimized.

Step 4: Generate a set of N solutions with dimension D between maximum and minimum limits of the control variables.

Step 5: Set $N^{inter} = 1$.

Step 6: Are network constraints satisfied? if Yes go to Step 7, if No go to Step 8.

Step 7: Calculate the values of objective functions (PFM and EMM) for all agents, then go to Step 9.

Step 8: Discard the results.

Step 9: Find the smallest fitness value (F_b) and related best solution ($X_{b,s}$).

Step 10: Calculate the probability of the fitness value (p_i^{rob}) based on Eqs. (2) and (4).

Step 11: Check if $p_i^{rob} \geqslant 0.5$, if Yes go to Step 12, otherwise go to Step 13.

Step 12: Use the operators of HHO, then go to Step 14.

Step 13: Use the operators of PSO as descripted in (PSO) Algorithm, then go to Step 14.

Step 14: Check if $M \geqslant i$, if Yes go to Step 16, otherwise jump to Step 15.

Step 15: $i = i + 1$, go to Step 6.

Step 16: Check if $N^{iter} \leqslant N^{iter,Max}$, if Yes go to Step 18, otherwise jump to Step 17.

Step 17: Set $N^{iter} = N^{iter+1}$, return to Step 6.

Step 18: Print the optimal results (objective functions values (PFM and EMM) HT, WP, PV, PSH and LS-EVs power).

Step 19: End.

10. Simulation Results and Analysis

10.1. Test sysetm

Many pieces of research concerning on the benefits of WP and PV systems have been conducted all over the world. The use of renewable energy sources like PV and WP is the main research area. Fig. 3 shows the plan for the combining various traditional HT and new WP, PV, PSH, and LS-EVs units.

The test system is the IEEE 118-bus network that includes 54 thermal (T) units that operate based on various fuels including 10 plants with crude oil, 11 units with gas and 33 plants with charcoal. As in Ref. [4], discusses eight hydro (H) units are employed to reach useful data and achieve acceptable performance. The linearization procedure, VLC and POZs highly impact the operation of thermal units. So, VLC is considered for plants 5, 10, 11, 28, 36, 43, 44 and 45 while POZs are adopted for plants 7, 10, 30, 34, 35 and 47. In general, this problem (M/S-O-DA-HTSS) is modeled in a two-stage (TS) framework. Fig. 4 illustrates the solution steps of the TS. The first stage involves problem estimation and the second stage deals with the operation of generation units formulated in a MIP framework. The outputs of the first stage consist of sizing and solving the planning problem for some inputs of the second stage. The solution to the second stage is found by employing the GAMS software, which is one of the popular optimization suites. The HHO helps solve the first stage problem, namely the planning problem. The planning decision variable in the first stage is a continuous variable for individual candidates, while it needs to be scaled so that a decision variable becomes an integer to be evaluated in the second stage. So, in this paper, an uncomplicated method is used for generating discrete decision variables. In the suggested approach, first, the main objective function is chosen to find the maximum expected profit (F_1). According to Refs. [29, 30], we solved the integration of HT, WP and PV units with stochastic multi-objective problem and found the feasible solutions. The M/S-O-HTSS with WP, PV, PSH and LS-EVs problem has also been solved here to reach the PFM of GenCos and EMM of T plants. Consequently, we analyze the impact of VLC, POZs, uncertain energy price, SR price and NSR price, load uncertainty, by neglecting the wind power uncertainty on the PFM and EMM. Four cases were considered to do analyses:

- **Case 1.** Stochastic multi-objective HTSS problem constaining WP, PV, PSH, EVs with VLC, POZs.
- **Case 2.** Stochastic single-objective HTSS problem constaining WP, PV, PSH, EVs with VLC, POZs.
- **Case 3.** Stochastic multi-objective HTSS problem constaining WP, PV, PSH, EVs with VLC.
- **Case 4.** Stochastic single-objective HTSS problem constaining WP, PV, PSH, EVs with VLC.

A) Stochastic MO-HTSS problem considering WP, PV, PSH, EVs with VLC, POZs

This part of the paper analyzes the optimization of the SMO-HTSS problem based on HHO-PSO algorithm to provide profit maximize (PFM) of GenCos and emission maximization (EMM). Also, the impact of of VLC, POZs, energy price uncertainty, WP, PV units uncertainty with PSH, EVs generation, SR and NSR price uncertainty on PFM and EMM is assessed. Table 2 reports the expected values of objective functions. The result of the first and second columns are related to the first and second objective functions (F_1 and F_2).

In Table 2, the the expected PFM and EMM found by applying the HHO-PSO are 2,760,585.20 ($) and 216,250.85 (lbs). Overall, T, H, WP, PV, PSH and LS-EVs units, SR and NSR produce 165675.66 (MW), 16311.27 (MW) and 332 (MW), 3580.42 (MW) and 2460.13 (MW) of electrical power, respectively. The remaining remark to note is that the computation time of solving the problem is 25 seconds. Figs. 5 and 6 show the convergence behavior of the HHO-PSO for PFM and EMM in the multi-objective optimization.

Planning report of GenCos and energy prices is depicted in Fig. 7. Also, expected energy price and profit obtained from applying the HHO-PSO are shown in Fig. 8. Fig. 9 illustrates the changes in the reservoir level for each hour. Fig. 10 provides the results of overall power output and demand in Case I.

B) Stochastic single-objective HTSS problem considering WP, PV, PSH, EVs with VLC, POZs

The SSO-HTSS problem is solved by applying the HHO-PSO so that the GenCos profit is maximized. Here we analyze the impact of VLC, POZs, energy price uncertainty, WP, PV units uncertainty with PSH, EVs generation, SR and NSR price uncertainty on the PFM. Maximum values of objective functions are reported in Table 3. As is observed, the expected profit that can be obtained by a stochastic solution to the HTSS problem considering WP, PV, PSH and LS-EVs with VLC, POZs will be 2550342.39 ($). The thermal, hydro and WP, PV, PSH, LS-EVs units, SR and NSR generate 165660.66 (MW), 16286.27 (MW) and 311 (MW), 3515.55 (MW), 2451.18 (MW) power. It is concluded that RERs not only impacts the profit and power outputs, but changes the SR and NSR of HT units.

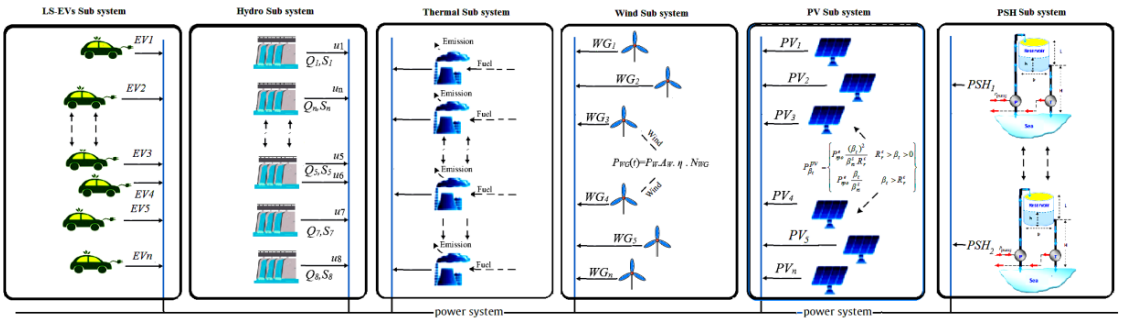

Fig. 3. The scheme of combining different traditional HT and new WP, PV, LS-EVs and PSH units.

Table 2. The HHO-PSO algorithm solution to the SMO-HTSS problem (WP, PV, PSH, LS-EVs with VLC, POZs).

F_1: Expected profit ($)	F_2: Expected emission (lbs)	Total power (MW)	Total reserve (MW)	Computation time (s)
2760585.20	216250.85	182318.93	6040.55	52

Table 3. The solution of the HHO-PSO algorithm to the SSO- HTSS problem (WP, PV, PSH, EVs with VLC, POZs).

Total power (MW)	Total reserve (MW)	F_1: Expected profit ($)	Computation time (s)
182257.27	5966.73	2550342.39	40

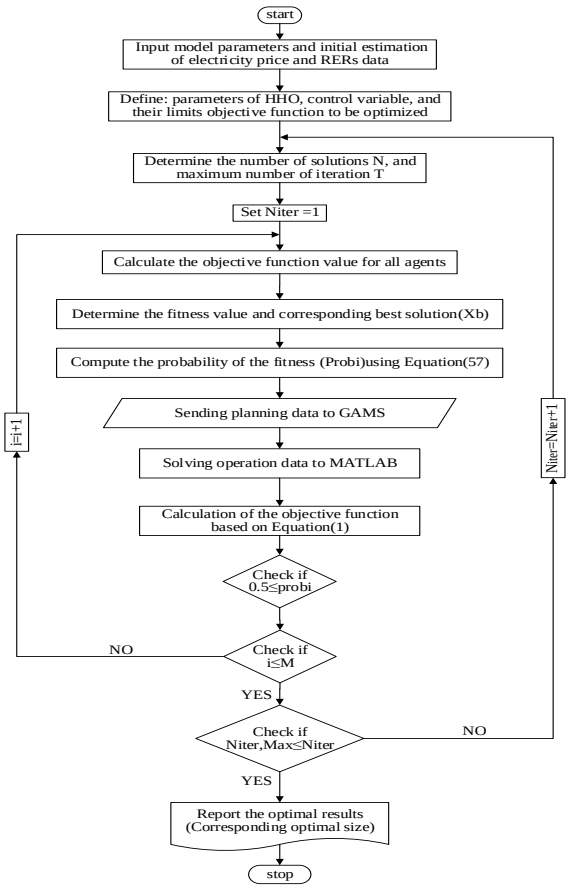

Fig. 4. Layout of the procedure used for modeling the two-stage together with uncertainty.

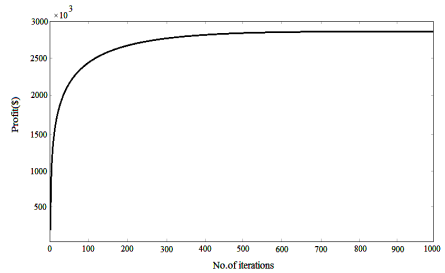

Fig. 5. The convergence behavior of the HHO-PSO for PFM in the multi-objective optimization.

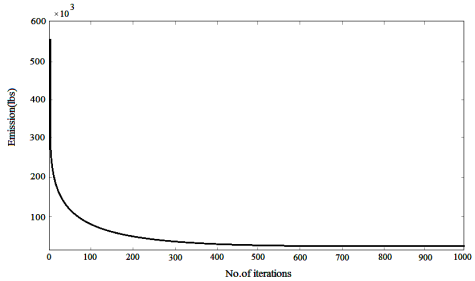

Fig. 6. The convergence behavior of the HHO-PSO method for EMM in the multi-objective optimization.

However, POZs of thermal units 7, 10, 30, 34, 35, and 45 are limited. Besides, as per Table 3, the sum of power and reserve is 182257.27 (MW) and 5966.73 (MW), and the computaiton time to solve the problem is 40 s, which is the optimal time based on the suggested HHO-PSO algorithm. However, Fig. 11 shows the convergence behvaior of the HHO-PSO when applied to the profit objective function in the single-objective optimization.

According to Fig. 12, the energy price and the amount of output power are correlated. Fig. 13 reports the energy price and expected profit (EP) for a day-ahead period. Figs. 14 and 15 illustrate the changes in reservoir storage and overall output power with load uncertainty curves. Nonetheless, when energy price rises, the power output is greater. When energy price is low, the power is

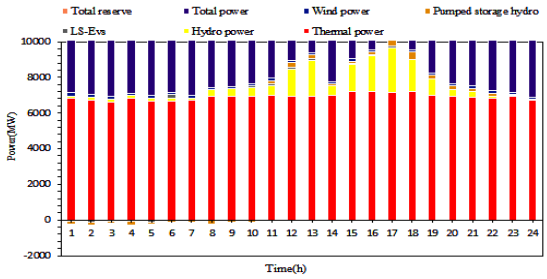

Fig. 7. The planning resultss of H, T power GenCos and energy price with using the HHO-PSO algorithm in the multi-objective optimization.

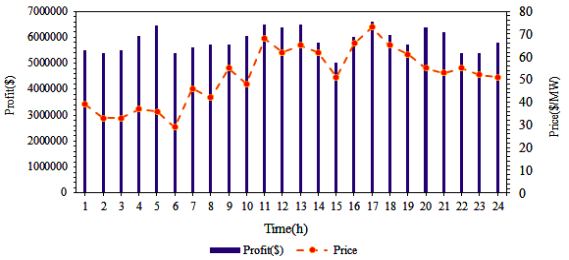

Fig. 8. The energy price and profit curves of GenCos with using the HHO-PSO algorithm in the multi-objective optimization.

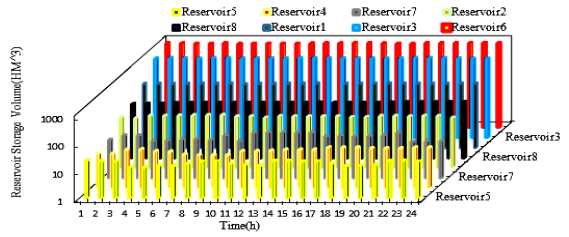

Fig. 9. Hourly reservoir storage volumes for Case 1.

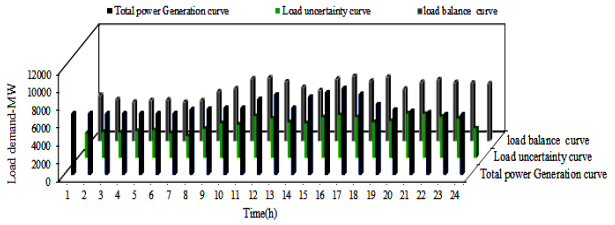

Fig. 10. Hourly total power generation and load uncertainty curves for Case 1.

low and water is stored so that the constraint on the ultimate water storage is met. Accordingly, RERs not only impact the profit and power output, but has effects on the SR and NSR of hydro-thermal generation units.

By reviewing sections 10.1.1 and 10.1.2 it can be concluded that generation by various power plant units in the multi-objective and single-objective stochastic planning is 182,318.93 (MW) and 182,257.27 (MW). The expected profit in each of these two sections is 2,760,585.20 ($) and 2,550,342.39 ($), respectively. In general, the difference between the generation and expected profit in these two cases (multi-objective and single-objective planning) is 61.66 MW and $210,242.81, which shows an increase in both of these items.

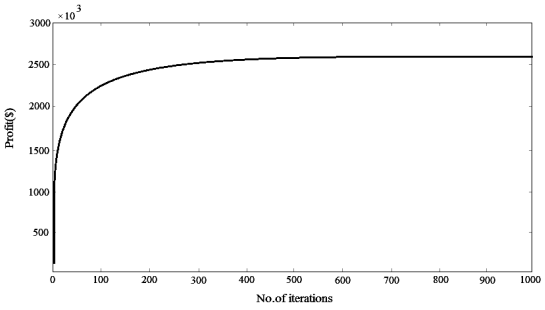

Fig. 11. The convergence behavior of the HHO-PSO method for the PFM in the single-objective optimization.

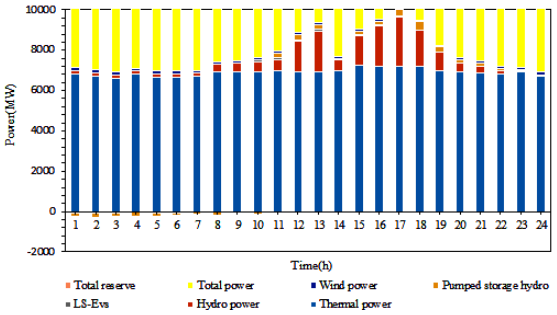

Fig. 12. The planning results of H, T, WP, PV, PSH and LS-EVs power GenCos and energy price.

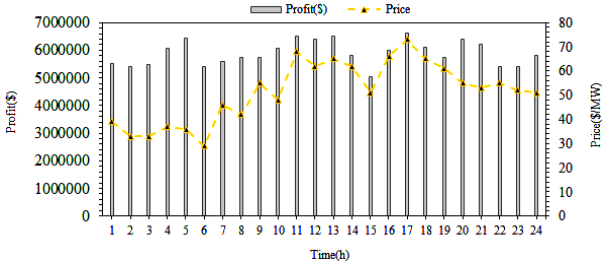

Fig. 13. The energy price and profit curves of GenCos.

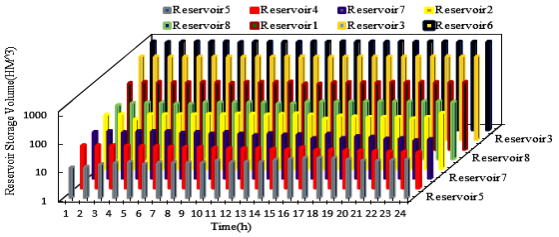

Fig. 14. Hourly reservoir storage volumes for Case 2.

C) Case 3: Stochastic multi-objective HTSS problem considering WP, PV, PSH, EVs with VLC

Optimization of the SMO-HTSS problem by adopting the HHO-PSO algorithm is presented here to find the maximum PFM of GenCos and minimum EMM. We also examine how VLC, energy price uncertainty WP, PV units uncertainty with PSH, EVs generation, SR and NSR price uncertainty impact the PFM and EMM. Table 4 reports the expected values of objective functions. Accordingly, the first and second columns correspond to the first and second objective functions (F_1 and F_2).

In Table 4, the expected values of objective functions, i.e.

Table 4. The solution of the HHO-PSO algorithm to the SMO- HTSS problem (WP, PV, PSH, LS-EVs with VLC, POZs).

F_1: Expected profit ($)	F_2: Expected emission (lbs)	Total power (MW)	Total reserve (MW)	Computation time (s)
2760608.49	216130.01	182407.48	6067.01	47

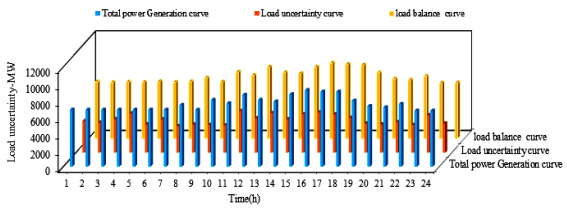

Fig. 15. Hourly total power generation and load uncertainty curves for Case 2.

expected profit and expected emission, achieved by employing the HHO-PSO show the predicted PFM and EMM of 2,760,608.49 ($) and 216,130.01 (lbs). Overall, the T, H, WP, PV, PSH and LS-EVs units, SR and NSR produce 165742.29 (MW), 16320.19 (MW), 345 (MW), 3593.32 (MW) and 2473.69 (MW) electrical power, respectively. The problem solution is found in 47 s. However, Figs. 16 and 17 depict the convergence behacvior of the HHO-PSO applied to PFM and EMM in the multi-objective optimization.

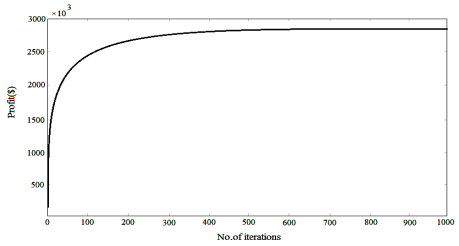

Fig. 16. The convergence behavior of the HHO-PSO for the PFM in the multi-objective optimization.

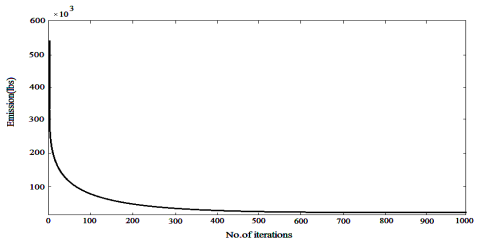

Fig. 17. The convergence behavior of the HHO-PSO for the EMM function in the multi-objectiv optimization.

Also, Fig. 18 reports the planning results of GenCos profit and energy prices. Fig. 19 presents energy price and EP for a day-ahead period when the HHO-PSO is applied. Also, Fig. 20 shows the hourly water level in the reservoir. Fig. 21 shows the hourly power output with load uncertainty curves for Case 3.

D) Case 4: Stochastic single-objective HTSS problem considering WP, PV, PSH, EVs with VLC

Optimization of the SSO-HTSS problem by applying the HHO-PSO algorithm is presented here to find maximum GenCos profit. Here we examine how VLC, energy price uncertainty WP, PV units uncertainty with PSH, EVs generation, SR and NSR price uncertainty impact the PFM. Table 5 reports the maximum values of objective functions. As is seen, the EP obtaiend from a

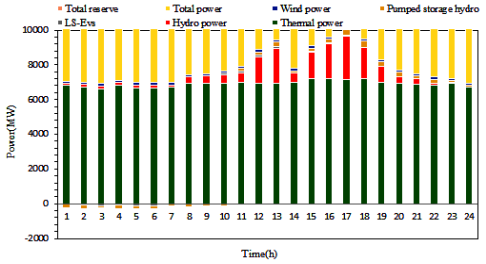

Fig. 18. The planning results of H,T power GenCos and energy price with using the HHO-PSO algorithm.

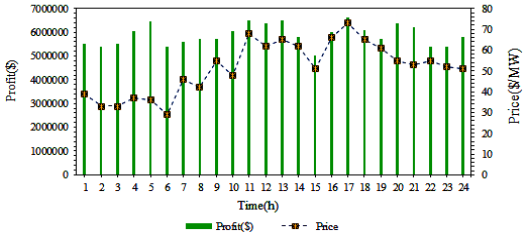

Fig. 19. Energy price and profit curves of GenCos with using the HHO-PSO algorithm.

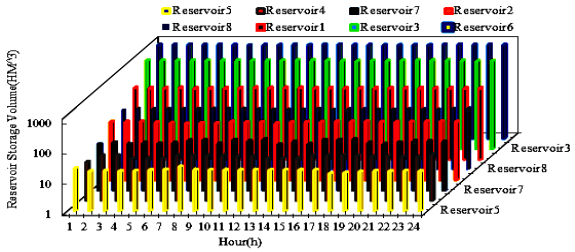

Fig. 20. Hourly water level for Case 3.

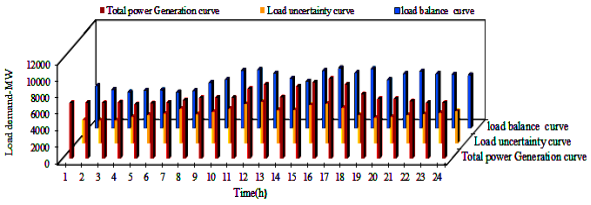

Fig. 21. Hourly overall power output and load uncertainty curves for Case 3.

stochastic solution to the HTSS problem considering WP, PV, PSH and LS- EVs with VLC will be 2550371.89 ($). Overall, the H, T, WP, PV, PSH and LS-EVs units, SR and NSR produce 165678.19 (MW),16297.55 (MW), 316 (MW), 3520.01 (MW), 2456.83 (MW) power. Accordingly, RERs not only impacts the profit and power ouput of generation units, but has has effects on SR and NSR of hydro-thermal generation units.

There are limits on the VLC of thermal units 7, 10, 30, 34, 35 and 45. Also, according to Table 5, the overall power is 182291.74 (MW), the overall reserve is 5976.93 (MW) and

Table 5. The solution of the HHO-PSO algorithm to the SSO- HTSS problem (WP, PV, PSH, EVs with VLC, POZs).

Total power (MW)	Total reserve (MW)	F_1: Expected profit ($)	Computation time (s)
182291.74	5976.93	2550371.89	33

computation time is 33 s, which is the optimal time obtained by the suggested HHO-PSO algorithm. However, Fig. 22 shows how the HHO-PSO optimization for profit objective function in single-objective optimization.

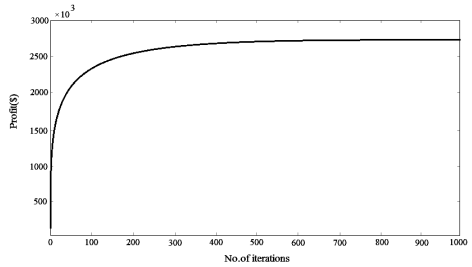

Fig. 22. The convergence behavior of the HHO-PSO for the PFM in single-objective optimization.

Fig. 23 shows that energy price and total output power of generation units are correlated. Fig. 24 presents the energy price and EP for a day-ahead period when the proposed algorithm is applied. Figs. 25 and 26 provide the water level per hour and the amount of power produced by all units. When energy price rises, the power output is greater. When energy price is low, the power is low and water is stored so that the constraint on the ultimate water storage is met. Accordingly, RERs not only impact the profit and power output, but has effects on the SR and NSR of hydro and thermal generation units.

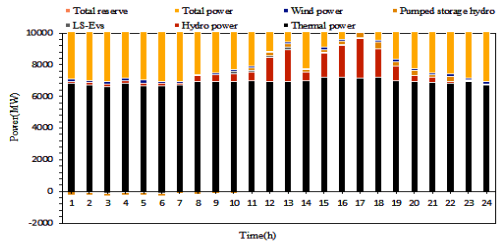

Fig. 23. The planning results of H, T, WP, PV, PSH and LS-EVs power GenCos and energy price.

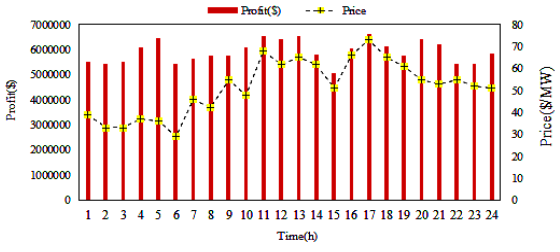

Fig. 24. The energy price and profit curves of GenCos.

However, by reviewing sections 10.1. C) and 10.1. D) respectively, it can be seen that the generation by different power plant units in multi-objective and single-objective stochastic planning is 182407.48 (MW) and 182291.74 (MW) respectively, while the expected profits in each of these sections are 2,760,608.49 ($) and 2,550,371.89 ($), respectively. In general, the difference between the generation of plants and the expected profit in

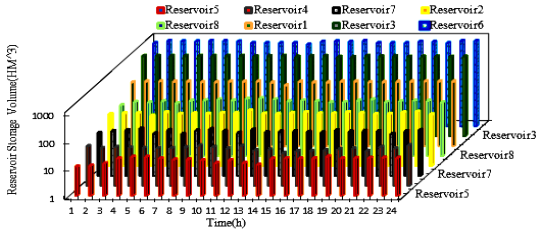

Fig. 25. Water level in the reservoir for Case 4.

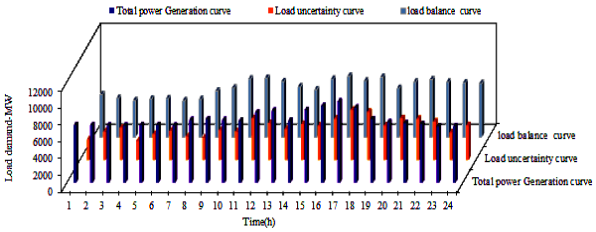

Fig. 26. Hourly overall power output and load uncertainty curves for Case 4.

multi-objective and single-objective planning is 115.74 (MW) and 210,236.60 ($), respectively, which indicates the increase in the both of these items. It is obvious that the profit from case studies given in sections 10.1. A) and 10.1. B) shows a decreasing trend compared to those of sections 10.1. C) and 10.1. D); this is caused by considering the effects of valve loading cost (VLC) and prohibited operation areas (POZs).

11. Comparative Analysis

The results obtained in previous sections are now comapred. Table 6 lists the values of objective functions (both multi and single objectives) concerning the PFM and EMM for four cases. As one can vividly observe, there are four case studies. Cases 1 and 3 are based on a multi-objective function and, Case1 has a total power capacity of 182318.93 (MW), expected profit of 2760585.20 ($) and emission level of 216250.85 (lbs), but Case 3 has a total power capacity of 182407.48 (MW), expected profit of 2760608.49 ($) and emission level of 216130.01 (lbs). Cases 2 and 4 are based on a single objective function. Case 2 has a total power capacity of 182257.27 (MW) and expected profit of 2550342.39 ($), but Case 4 has a total power capacity of 182291.74 (MW) and the expected profit is 2550371.89 ($). The main reference is to the important conclusion that can be drawn from the results of Table 7, and that is the effect of considering and not considering POZs with and without VLC in each of the study cases, followed by the effects that will have on profit and emission values. The paper showed that energy GenCos are able to achieve PFM and EMM by adopting renewables like WP, PV, PSH and LS-EVs. So, the HHO-PSO outperforms its counterpart methods (ε-constraint) or optimization techniques (ALO, HHO) in terms of reaching the optimization purposes.

In addition, Table 7 also shows the generation unit type, objective function, etc., and compares the present research with prior studies. For a general review of the references, one can refer to each of them using Table 7 and notice important remarks. Ref. [31], refers to the coordination of hydro, thermal, wind and photovoltaic power plant units by considering the multi-objective function, the second case study, the most important of which is the maximization of clean energy in addition to the network load level and the aoption of only one algorithm in solving the problem. Ref. [35], refers to the coordination of hydro, wind and photovoltaic power plant units by considering the multi-objective function, the fourth case studies, to minimize costs and emission level using

Table 6. Results of four cases.

Case study	Type objective	Total power (MW)	Total reserve (MW)	E^*.profit ($)	E^*. emission (lbs)	C^*.time (s)
Case 1	Multi-objective	182318.93	6040.55	2760585.20	216250.85	52
Case 2	Single-objective	182257.27	5966.73	2550342.39	-	40
Case 3	Multi-objective	182407.48	6067.01	2760608.49	216130.01	47
Case 4	Single-objective	182291.74	5976.93	2550371.89	-	33

E^*:Expected; C^*:Computation

Table 7. A report on some literature focused on hybrid (HT, WP, PV, etc.) energy systems.

Description	**Our article**	**Ref. [44]**	**Ref. [43]**	**Ref. [37]**	**Ref. [35]**	**Ref. [31]**
Generation unit type	H,T, WP, PV, PSH, LS-EVs	WP, T, PV	H,T, WP, CGP, REB	WP, PV, BATTERY	H, PV, WP	H,T,WP, PV
Multi-objective function	✓	✓	✓	✓	✓	✓
Single-objective function	✓	✗	✗	✗	✗	✗
Uncertainty number	5	3	1	3	2	2
Max. profit	✓	✓	✓	✗	✗	✗
Min. emission	✓	✓	✗	✓	✓	✗
Min. cost	✗	✗	✗	✓	✓	✗
Max. clean energy	✗	✗	✗	✗	✗	✓
Min. the fluctuation of load	✗	✗	✗	✗	✗	✓
Case study number	4	2	4	2	4	2
Uncertainty modeling	✓	✓	✓	✓	✓	✓
Simulate random method	✓	✗	✗	✓	✗	✓
Algorithm	✓	✗	✗	✗	✓	✓
Other optimization	✗	✗	✗	✗	✗	✗
Consider the load	✓	✗	✗	✗	✗	✓
Solution method	HHO-PSO	WST	✗	CCP, FMP	MBFA	MOCS
Operation	GENCOs	GENCOs	GENCOs	GENCOs	GENCOs	GENCOs
Combination algorithm	✓	✗	✗	✗	✗	✗

Table 8. Results of Refs. [53], [54], [55] for comparative analysis.

Reference	**Case study**	**Type objective**	**Generation unit type**	**Considering factors**	**Expected profit ($)**	**Expected emission (lbs)**	**Solution method**
Ref. [53]	Case 1	Single-objective	HT	VLC, POZs	5,419,857.42	-	MIP
	Case 2	Single-objective	HT-WP	VLC, POZs	5,841,292.48	-	MIP
	Case 1	Single-objective	HT	VLC, POZs	5,419,896.15	-	Antlion*Op-Algo
	Case 2	Single-objective	HT	-	5,665,420.53	-	Antlion*Op-Algo
Ref. [54]	Case 3	Single-objective	HT-WP	VLC, POZs	5,419,915.40	-	Antlion*Op-Algo
	Case 4	Single-objective	HT-WP	-	5,841,301.22	-	Antlion*Op-Algo
	Case 5	Single-objective	HT-WP-PV	VLC, POZs	5,421,812.19	-	Antlion*Op-Algo
	Case 6	Single-objective	HT-WP-PV-SH	-	5,841,383.53	-	Antlion*Op-Algo
Ref. [55].	Case 1	Single-objective	HT-WP-PV-SH-PHS	VLC, POZs	5,421,648.01	-	HHO*Op-Algo
	Case 2	Single-objective	HT-WP-PV-SH-PHS	-	5,843,083.07	-	HHO*Op-Algo
	Case 3	Single-objective	HT-WP-PV-SH-PHS	VLC	5,424,418.01	-	HHO*Op-Algo
	Case 4	Single-objective	HT-WP-PV-SH-PHS	-	5,845,853.17	-	HHO*Op-Algo
Our article	Case 1	Multi-objective	HT-WP-PV-PHS-EVs	VLC, POZs	2,760,585.20	216,250.85	HHO-PSO*Op-Algo
	Case 2	Single-objective	HT-WP-PV-PHS-EVs	VLC, POZs	2,550,342.39	-	HHO-PSO*Op-Algo
	Case 3	Multi-objective	HT-WP-PV-PHS-EVs	VLC	2,760,608.49	216,130.01	HHO-PSO*Op-Algo
	Case 4	Single-objective	HT-WP-PV-PHS-EVs	VLC	2,550,371.89	-	HHO-PSO*Op-Algo

only one algorithm. Ref. [37], refers to the coordination of battery, PV, WP power plant units by considering the multi-objective function (second case study), which minimizes costs and emission. Ref. [43], deals with the coordination of H, T, WP, CGP, REB power plant units by considering the multi-objective function, the fourth case study, which refers to the maximization of profit in solving the problem. Ref. [44], addresses the coordination of WP, T, PV power plant units by considering the multi-objective function, the second, which refers to the maximization of profit and minimization of emission in solving the problem.

In the following, Refs. [53], [54], [55] which are summarized in Table 8 can be referred to for further review and comparison. Ref. [53] has used the participation of H, T, WP units and the MIP solution method with the help of a single objective function for two study cases in order to maximize profit. Ref. [54] adopted H, T, WP, PV, SH units and the Antlion optimization algorithm solution method with the help of a single objective function, for six study cases to maximize the profit. Ref. [55] investigates the participation of H, T, WP, PV, SH, PHS units and the Harris hawks optimization algorithm with the help of single objective function for four case studies in order to maximize profit. In the following, it can be said that the framework and structure of the stated references are almost similar to our presented article, but among them, according to the type of participation of generation units and other parameters, Ref. [55] deals with study cases 1 and 3, where the profit from their single objective function is equal to $5421648.01 and $5424418.01, respectively. Meanwhile, the profit from the single objective function in the study cases 1 and 4 of our article is equal to $2550342.39 and $2550371.89, respectively. As can be seen, there is a significant difference between the profit obtained in the study cases of our article and Ref. [55], which is caused by factors such as: the conditions governing the selection and type of power plant units, the type of selection algorithm, energy price values , uncertainty values in the power of renewable energy sources, etc. It should be noted that there is no reference to the multi-objective function in any of the discussed references, so it is not possible to accurately compare the numerical results obtained from the study cases with this article.

However, in the current research, some renewable energie sources and uncertainties are consdiered, and the HHO-PSO algorithm is adopted to solve the HTSS problem with WP, PV, PSH and LS-EVs power considering the stochastic variable, where two objective functions are employed for PFM and EMM. Also, the use of the proposed method (HHO-PSO algorithm) has accelerated finding the solution to the problems.

12. CONCLUSION

A novel algorithm, named HHO-PSO, is introduced by integrating the MO-HTSS to address the uncertainties and intermittent outputs of wind and solar power, pumped storage hydro (PSH), and large-scale electric vehicles (LS-EVs). The proposed approach, which incorporates uncertain parameters in the scheduling of units, helps GenCos manage the variability of certain factors, including energy prices and output power of generation units. This approach allows GenCos to maximize revenue while minimizing emissions. Two objective functions, profit maximization and emission minimization, were optimized using the introduced method. By managing the uncertain output of renewables effectively, GenCos can significantly benefit from operating generation units and make informed decisions on other aspects of the system. The results obtained from applying the proposed method to four case studies validate its effectiveness and demonstrate the capability of this approach.

REFERENCES

[1] A. J. Wood, B. F. Wollenberg, and G. B. Sheblé, *Power generation, operation, and control*. John Wiley & Sons, 2013.

[2] S. Bisanovic, M. Hajro, and M. Dlakic, "Hydrothermal self-scheduling problem in a day-ahead electricity market," *Electr. Power Syst. Res.*, vol. 78, no. 9, pp. 1579–1596, 2008.

[3] I. Farhat and M. El-Hawary, "Optimization methods applied for solving the short-term hydrothermal coordination problem," *Electr. Power Syst. Res.*, vol. 79, no. 9, pp. 1308–1320, 2009.

[4] A. J. Conejo, J. M. Arroyo, J. Contreras, and F. A. Villamor, "Self-scheduling of a hydro producer in a pool-based electricity market," *IEEE Trans. Power Syst.*, vol. 17, no. 4, pp. 1265–1272, 2002.

[5] A. M. Foley, P. G. Leahy, K. Li, E. McKeogh, and A. P. Morrison, "A long-term analysis of pumped hydro storage to firm wind power," *Appl. Energy*, vol. 137, pp. 638–648, 2015.

[6] J. Dhillon, S. Parti, and D. Kothari, "Fuzzy decision-making in stochastic multiobjective short-term hydrothermal scheduling," *IEE Proc.-Gener. Transm. Distrib.*, vol. 149, no. 2, pp. 191–200, 2002.

[7] M. R. Norouzi, A. Ahmadi, A. M. Sharaf, and A. E. Nezhad, "Short-term environmental/economic hydrothermal scheduling," *Electr. Power Syst. Res.*, vol. 116, pp. 117–127, 2014.

[8] A. Ahmadi, J. Aghaei, H. A. Shayanfar, and A. Rabiee, "Mixed integer programming of multiobjective hydro-thermal self scheduling," *Appl. Soft Comput.*, vol. 12, no. 8, pp. 2137–2146, 2012.

[9] M. Izadbakhsh, M. Gandomkar, A. Rezvani, and A. Ahmadi, "Short-term resource scheduling of a renewable energy based micro grid," *Renewable Energy*, vol. 75, pp. 598–606, 2015.

[10] J. Catalão, H. Pousinho, and J. Contreras, "Optimal hydro scheduling and offering strategies considering price uncertainty and risk management," *Energy*, vol. 37, no. 1, pp. 237–244, 2012.

[11] F. Partovi, M. Nikzad, B. Mozafari, and A. M. Ranjbar, "A stochastic security approach to energy and spinning reserve scheduling considering demand response program," *Energy*, vol. 36, no. 5, pp. 3130–3137, 2011.

[12] C.-L. Tseng and W. Zhu, "Optimal self-scheduling and bidding strategy of a thermal unit subject to ramp constraints and price uncertainty," *IET Gener. Transm. Distrib.*, vol. 4, no. 2, pp. 125–137, 2010.

[13] M. Li, Y. Li, and G. Huang, "An interval-fuzzy two-stage stochastic programming model for planning carbon dioxide trading under uncertainty," *Energy*, vol. 36, no. 9, pp. 5677–5689, 2011.

[14] A. Ahmadi, M. Charwand, and J. Aghaei, "Risk-constrained optimal strategy for retailer forward contract portfolio," *Int. J. Electr. Power Energy Syst.*, vol. 53, pp. 704–713, 2013.

[15] K. Meng, H. G. Wang, Z. Dong, and K. P. Wong, "Quantum-inspired particle swarm optimization for valve-point economic load dispatch," *IEEE Trans. Power Syst.*, vol. 25, no. 1, pp. 215–222, 2009.

[16] J. Aghaei, A. Ahmadi, A. Rabiee, V. G. Agelidis, K. M. Muttaqi, and H. A. Shayanfar, "Uncertainty management in multiobjective hydro-thermal self-scheduling under emission considerations," *Appl. Soft Comput.*, vol. 37, pp. 737–750, 2015.

[17] T. Li and M. Shahidehpour, "Dynamic ramping in unit commitment," *IEEE Trans. Power Syst.*, vol. 22, no. 3, pp. 1379–1381, 2007.

[18] Y. Li, Q. Wu, M. Li, and J. Zhan, "Mean-variance model for power system economic dispatch with wind power integrated," *Energy*, vol. 72, pp. 510–520, 2014.

[19] X. Yuan, B. Ji, S. Zhang, H. Tian, and Z. Chen, "An improved artificial physical optimization algorithm for dynamic dispatch of generators with valve-point effects and wind power," *Energy Convers. Manage.*, vol. 82, pp. 92–105, 2014.

[20] H. M. Dubey, M. Pandit, and B. Panigrahi, "Hybrid flower pollination algorithm with time-varying fuzzy selection mechanism for wind integrated multi-objective dynamic economic dispatch," *Renewable Energy*, vol. 83, pp. 188–202, 2015.

[21] X. Yuan, H. Tian, Y. Yuan, Y. Huang, and R. M. Ikram, "An extended nsga-iii for solution multi-objective hydro-thermal-wind scheduling considering wind power cost," *Energy Convers. Manage.*, vol. 96, pp. 568–578, 2015.

[22] J. Zhou, P. Lu, Y. Li, C. Wang, L. Yuan, and L. Mo, "Short-term hydro-thermal-wind complementary scheduling considering uncertainty of wind power using an enhanced multi-objective bee colony optimization algorithm," *Energy Convers. Manage.*, vol. 123, pp. 116–129, 2016.

[23] X. Yuan, H. Tian, Y. Yuan, Y. Huang, and R. M. Ikram, "An extended nsga-iii for solution multi-objective hydro-thermal-wind scheduling considering wind power cost," *Energy Convers. Manage.*, vol. 96, pp. 568–578, 2015.

[24] S. Mirjalili, "The ant lion optimizer," *Adv. Eng. Software*, vol. 83, pp. 80–98, 2015.

[25] H. M. Dubey, M. Pandit, and B. Panigrahi, "Hydro-thermal-wind scheduling employing novel ant lion optimization technique with composite ranking index," *Renewable Energy*, vol. 99, pp. 18–34, 2016.

[26] A. Wijesinghe and L. L. Lai, "Small hydro power plant analysis and development," in *2011 4th Int. Conf. Electr. Util. Deregulation Restructuring Power Technol.*, pp. 25–30, IEEE, 2011.

[27] M. Baneshi and F. Hadianfard, "Techno-economic feasibility of hybrid diesel/pv/wind/battery electricity generation systems for non-residential large electricity consumers under southern iran climate conditions," *Energy Convers. Manage.*, vol. 127, pp. 233–244, 2016.

[28] F.-F. Li and J. Qiu, "Multi-objective optimization for integrated hydro–photovoltaic power system," *Appl. Energy*, vol. 167, pp. 377–384, 2016.

[29] Z. Ding, H. Hou, G. Yu, E. Hu, L. Duan, and J. Zhao, "Performance analysis of a wind-solar hybrid power generation system," *Energy Convers. Manage.*, vol. 181, pp. 223–234, 2019.

[30] X. Wang, J. Chang, X. Meng, and Y. Wang, "Hydro-thermal-wind-photovoltaic coordinated operation considering the comprehensive utilization of reservoirs," *Energy Convers. Manage.*, vol. 198, p. 111824, 2019.

[31] X. Wang, J. Chang, X. Meng, and Y. Wang, "Short-term hydro-thermal-wind-photovoltaic complementary operation of

interconnected power systems," *Appl. Energy*, vol. 229, pp. 945–962, 2018.
[32] A. Zakaria, F. B. Ismail, M. H. Lipu, and M. A. Hannan, "Uncertainty models for stochastic optimization in renewable energy applications," *Renewable Energy*, vol. 145, pp. 1543–1571, 2020.
[33] L. Wu, M. Shahidehpour, and T. Li, "Stochastic security-constrained unit commitment," *IEEE Trans. Power Syst.*, vol. 22, no. 2, pp. 800–811, 2007.
[34] X. Wang, Y. Mei, Y. Kong, Y. Lin, and H. Wang, "Improved multi-objective model and analysis of the coordinated operation of a hydro-wind-photovoltaic system," *Energy*, vol. 134, pp. 813–839, 2017.
[35] A. Panda, U. Mishra, M.-L. Tseng, and M. H. Ali, "Hybrid power systems with emission minimization: Multi-objective optimal operation," *J. Cleaner Prod.*, vol. 268, p. 121418, 2020.
[36] S. Mandal, B. K. Das, and N. Hoque, "Optimum sizing of a stand-alone hybrid energy system for rural electrification in bangladesh," *J. Cleaner Prod.*, vol. 200, pp. 12–27, 2018.
[37] J.-Y. Lee, K. B. Aviso, and R. R. Tan, "Multi-objective optimisation of hybrid power systems under uncertainties," *Energy*, vol. 175, pp. 1271–1282, 2019.
[38] E. Rakhshani, H. Mehrjerdi, and A. Iqbal, "Hybrid wind-diesel-battery system planning considering multiple different wind turbine technologies installation," *J. Cleaner Prod.*, vol. 247, p. 119654, 2020.
[39] S. Yao, S. Zhang, and X. Zhang, "Renewable energy, carbon emission and economic growth: A revised environmental kuznets curve perspective," *J. Cleaner Prod.*, vol. 235, pp. 1338–1352, 2019.
[40] M. Simab, M. S. Javadi, and A. E. Nezhad, "Multi-objective programming of pumped-hydro-thermal scheduling problem using normal boundary intersection and vikor," *Energy*, vol. 143, pp. 854–866, 2018.
[41] P. Aliasghari, B. Mohammadi-Ivatloo, M. Alipour, M. Abapour, and K. Zare, "Optimal scheduling of plug-in electric vehicles and renewable micro-grid in energy and reserve markets considering demand response program," *J. Cleaner Prod.*, vol. 186, pp. 293–303, 2018.
[42] O. Abedinia, M. Zareinejad, M. H. Doranehgard, G. Fathi, and N. Ghadimi, "Optimal offering and bidding strategies of renewable energy based large consumer using a novel hybrid robust-stochastic approach," *J. Cleaner Prod.*, vol. 215, pp. 878–889, 2019.
[43] L. Ju, Q. Tan, R. Zhao, S. Gu, W. Wang, *et al.*, "Multi-objective electro-thermal coupling scheduling model for a hybrid energy system comprising wind power plant, conventional gas turbine, and regenerative electric boiler, considering uncertainty and demand response," *J. Cleaner Prod.*, vol. 237, p. 117774, 2019.
[44] H. Khaloie, A. Abdollahi, M. Shafie-Khah, P. Siano, S. Nojavan, A. Anvari-Moghaddam, and J. P. Catalão, "Co-optimized bidding strategy of an integrated wind-thermal-photovoltaic system in deregulated electricity market under uncertainties," *J. Cleaner Prod.*, vol. 242, p. 118434, 2020.
[45] M. A. Ramli, H. Bouchekara, and A. S. Alghamdi, "Optimal sizing of pv/wind/diesel hybrid microgrid system using multi-objective self-adaptive differential evolution algorithm," *Renewable Energy*, vol. 121, pp. 400–411, 2018.
[46] Y. Shen and H. Yang, "Multi-objective optimization of integrated solar-driven co2 capture system for an industrial building," *Sustainability*, vol. 15, no. 1, p. 526, 2022.
[47] X. Wu, B. Liao, Y. Su, and S. Li, "Multi-objective and multi-algorithm operation optimization of integrated energy system considering ground source energy and solar energy," *Int. J. Electr. Power Energy Syst.*, vol. 144, p. 108529, 2023.
[48] J. A. Concha-Carrasco, M. A. Vega-Rodríguez, and C. J. Pérez, "A multi-objective artificial bee colony approach for profit-aware recommender systems," *Inf. Sci.*, vol. 625, pp. 476–488, 2023.
[49] R. Mena, M. Godoy, C. Catalán, P. Viveros, and E. Zio, "Multi-objective two-stage stochastic unit commitment model for wind-integrated power systems: A compromise programming approach," *Int. J. Electr. Power Energy Syst.*, vol. 152, p. 109214, 2023.
[50] Y. Ding, Q. Tan, Z. Shan, J. Han, and Y. Zhang, "A two-stage dispatching optimization strategy for hybrid renewable energy system with low-carbon and sustainability in ancillary service market," *Renewable Energy*, vol. 207, pp. 647–659, 2023.
[51] S. Adhvaryyu, S. Prabhakar, and P. K. Adhvaryyu, "Multi objective short term hydro-thermal-chp scheduling using social spider algorithm," *Results Eng.*, vol. 16, p. 100586, 2022.
[52] C. Paul, P. K. Roy, and V. Mukherjee, "Wind and solar based multi-objective hydro-thermal scheduling using chaotic-oppositional whale optimization algorithm," *Electr. Power Compon. Syst.*, vol. 51, no. 6, pp. 568–592, 2023.
[53] M. Behnamfar, H. Barati, and M. Karami, "Stochastic short-term hydro-thermal scheduling based on mixed integer programming with volatile wind power generation," *J. Oper. Autom. Power Eng.*, vol. 8, no. 3, pp. 195–208, 2020.
[54] M. Behnamfar, H. Barati, and M. Karami, "Antlion optimization algorithm for optimal self-scheduling unit commitment in power system under uncertainties," *J. Oper. Autom. Power Eng.*, vol. 9, no. 3, pp. 226–241, 2021.
[55] M. Behnamfar and M. Abasi, "Uncertainty management in short-term self-scheduling unit commitment using harris hawks optimization algorithm," *J. Oper. Autom. Power Eng.*, vol. 12, no. 4, pp. 280–295, 2024.
[56] V. Vahidinasab and S. Jadid, "Stochastic multiobjective self-scheduling of a power producer in joint energy and reserves markets," *Electr. Power Syst. Res.*, vol. 80, no. 7, pp. 760–769, 2010.
[57] T. Li and M. Shahidehpour, "Price-based unit commitment: A case of lagrangian relaxation versus mixed integer programming," *IEEE Trans. Power Syst.*, vol. 20, no. 4, pp. 2015–2025, 2005.
[58] L. Wu, M. Shahidehpour, and T. Li, "Cost of reliability analysis based on stochastic unit commitment," *IEEE Trans. Power Syst.*, vol. 23, no. 3, pp. 1364–1374, 2008.
[59] N. Amjady, J. Aghaei, and H. A. Shayanfar, "Stochastic multiobjective market clearing of joint energy and reserves auctions ensuring power system security," *IEEE Trans. Power Syst.*, vol. 24, no. 4, pp. 1841–1854, 2009.
[60] I. G. Damousis, A. G. Bakirtzis, and P. S. Dokopoulos, "A solution to the unit-commitment problem using integer-coded genetic algorithm," *IEEE Trans. Power Syst.*, vol. 19, no. 2, pp. 1165–1172, 2004.
[61] Z. Michalewicz, *Genetic algorithms+ data structures= evolution programs*. Springer Science & Business Media, 2013.
[62] J. Garcia-Gonzalez, R. M. R. de la Muela, L. M. Santos, and A. M. Gonzalez, "Stochastic joint optimization of wind generation and pumped-storage units in an electricity market," *IEEE Trans. Power Syst.*, vol. 23, no. 2, pp. 460–468, 2008.
[63] Y. Zhang, J. Le, X. Liao, F. Zheng, K. Liu, and X. An, "Multi-objective hydro-thermal-wind coordination scheduling integrated with large-scale electric vehicles using imopso," *Renewable Energy*, vol. 128, pp. 91–107, 2018.
[64] A. A. Heidari, S. Mirjalili, H. Faris, I. Aljarah, M. Mafarja, and H. Chen, "Harris hawks optimization: Algorithm and applications," *Future Gener. Comput. Syst.*, vol. 97, pp. 849–872, 2019.
[65] M. R. Elkadeem, M. Abd Elaziz, Z. Ullah, S. Wang, and S. W. Sharshir, "Optimal planning of renewable energy-integrated distribution system considering uncertainties," *IEEE Access*, vol. 7, pp. 164887–164907, 2019.